W71-06245

WATER POLLUTION CONTROL RESEARCH SERIES • 16080 DWP 11/70

PB 198 220

Induced Air Mixing of Large Bodies of Polluted Water

Reproduced by
NATIONAL TECHNICAL
INFORMATION SERVICE
Springfield, Va. 22151

ENVIRONMENTAL PROTECTION

– about our cover

The cover illustration depicts a city in which man's activities coexist in harmony with the natural environment. The Water Quality Control Research Program has as its objective the development of the water quality control technology that will make such cities possible. Previously issued reports on the Water Quality Control Research Program include:

Report Number	Title/Author
16080DROC0/69	Stratified Reservoir Currents; by Oregon State Univ., Corvallis, Ore.
16080——06/69	Hydraulic and Mixing Characteristics of Suction Manifolds; by Univ. of Wash., Seattle, Wash.
16080——10/69	Nutrient Removal from Enriched Waste Effluent by the Hydroponic Culture of Cool Season Grasses; by Jas. P. Law. Robt. S. Kerr Water Res. Ctr., Ada, Okla.
16080——11/69	Nutrient Removal from Cannery Wastes by Spray Irrigation of Grassland; by Robt. S. Kerr Water Res. Ctr., Ada, Okla.

1 Accession Number	2 Subject Field & Group	SELECTED WATER RESOURCES ABSTRACTS INPUT TRANSACTION FORM
W71-06245	05G	

5 Organization

University of Maine, Orono, ~~Maine 04473~~

6 Title

INDUCED AIR MIXING OF LARGE BODIES OF POLLUTED WATER

10 Author(s)

Stefan A. Zieminski
and
Raymond C. Whittemore

16 Project Designation

~~16080DWP 11/70~~ A

21 Note

Copy available from GPO Sup Doc AS I 67.13/4: 16080DWP ~~11/70~~ , $.60 ; microfiche from NTIS as PB 198 220 , $0.95.

22 Citation

EPA-WQO Report No 16080 DWP, Nov 1970, 46p, 32fig, 5tab, 26ref

23 Descriptors (Starred First)

Aeration, Water Quality Control,* Air Entrainment, ~~Air Bubbles~~, Coalescence
Bubbles, Mixing, Diffusion, Tracers

25 Identifiers (Starred First)

Air Plume, ~~Diffusion, Bubble Size~~, Energy Input, ~~Mixing, Tracer, Mixing time~~.

27 Abstract

~~The work discussed in this report constitutes the Phase I of the investigation of~~ induced air mixing of large bodies of water was investigated. The objective ~~of this work~~ was to conduct a pilot-scale study to estimate the effects of variables such as the air flow rate, geometry of the body of water, energy input, size of air bubbles, and the pumping capacity of the air plume on the time of mixing. The latter was defined as the time required to reach 90% of the equilibrium concentration of the KCl tracer. In the study emphasis was put on the direction and relative magnitudes of the variables in order to obtain guidelines for large-scale investigation. Considerable time was spent on the development of the various experimental techniques. The tests were conducted in a plexiglas tank of 180 gallons capacity. It is stressed that the induced air system was investigated only from the viewpoint of its mixing performance. Its effect on aquatic life was not considered ~~in this work~~.

Abstractor: S. A. Zieminski

Institution: University of Maine, Orono, Maine 04473

WR:102 (REV. JULY 1969)
WRSIC

SEND TO: WATER RESOURCES SCIENTIFIC INFORMATION CENTER
U.S. DEPARTMENT OF THE INTERIOR
WASHINGTON, D. C. 20240

* GPO: 1969-359-339

Induced Air Mixing of Large Bodies of Polluted Water

by

Stefan A. Zieminski

and

Raymond C. Whittemore

Chemical Engineering Department

University of Maine

Orono, Maine 04473

for the

ENVIRONMENTAL PROTECTION AGENCY

WATER QUALITY OFFICE

Program #16080 DWP

November 1970

For sale by the Superintendent of Documents, U.S. Government Printing Office, Washington, D.C. 20402 - Price 60 cents

WQO Review Notice

This report has been reviewed by the Water Quality Office and approved for publication. Approval does not signify that the contents necessarily reflect the views and policies of the Water Quality Office, nor does mention of trade names or commercial products constitute endorsement or recommendation for use.

Abstract

The work discussed in this report constitutes the Phase I of the investigation of induced air mixing of large bodies of water. The objective of this work was to conduct a pilot scale study to estimate the effects of variables such as the air flow rate, geometry of the body of water, energy input, size of air bubbles, and the pumping capacity of the air plume on the time of mixing. The latter was defined as the time required to reach 90% of the equilibrium concentration of the KCl tracer. In the study emphasis was put on the direction and relative magnitudes of the variables in order to obtain guidelines for large-scale investigation. Considerable time was spent on the development of the various experimental techniques. The tests were conducted in a plexiglas tank of 180 gallons capacity. It is stressed that the induced air system was investigated only from the viewpoint of its mixing performance. Its effect on aquatic life was not considered in this work.

This report was submitted in fulfillment of project #16080 DWP under the sponsorship of the Federal Water Pollution Control Administration.

Key Words: Air Plume, Diffusion, Dispersion, Bubble Size, Energy Input, Mixing, Mixing Time, Tracer.

Contents

Section		Page
	Conclusions	vi
	Recommendations	viii
I	Introduction	1
II	Equipment and Operational Procedures	5
III	Discussion of Results	23
IV	References	45

List of Figures

		Page
Figure 1	Test Equipment.	3
Figure 2	Photograph of Test Equipment.	5
Figure 3	Photograph of Restricted System	6
Figure 4	Photograph of Air Bubbles	8
Figure 5	Photograph of Air Plume	8
Figure 6	Photograph of the Rising Disturbance of the Plume . .	10
Figure 7	Photograph of Anemometer in Calibrator.	12
Figure 8	Pumping Action of Plume	13
Figure 9	Photograph of Water Velocity Determination by Stroboscopic Photography	14
Figure 10	Photograph of Liquid Tracer Introduction.	15
Figure 11	Conductivity Cell Locations	16
Figure 12	Conductivity vs. Time Chart (Solution Tracer Introduction).	17
Figure 13	Photograph of Solid Tracer Introduction	18
Figure 14	Conductivity vs. Time (Solid Tracer Introduction. . .	20
Figure 15	Conductivity vs. Time (Continuous Tracer Introduction).	21
Figure 16	Mixing Time vs. Air Rate (Solution Tracer).	24
Figure 17	Mixing Time vs. Air Flow Rate (Solid Tracer).	25
Figure 18	Photograph of Circulation Pattern (Solution Tracer, 10 seconds).	28
Figure 19	Photograph of Circulation Pattern (Solution Tracer, 30 seconds).	28
Figure 20	Photograph of Circulation Pattern (Solution Tracer, 1 minute)	29

List of Figures (continued)

		Page
Figure 21	Photograph of Circulation Pattern (Solution Tracer, 2 minutes)	29
Figure 22	Photograph of Circulation Pattern (Solution Tracer, 3 minutes)	30
Figure 23	Stack Flow vs. Air Flow Rate.	31
Figure 24	Photograph of Circulation Pattern (Solid Tracer, 10 seconds).	32
Figure 25	Photograph of Circulation Pattern (Solid Tracer, 30 seconds).	32
Figure 26	Photograph of Circulation Pattern (Solid Tracer, 1 minute).	33
Figure 27	Photograph of Circulation Pattern (Solid Tracer, 2 minutes)	33
Figure 28	Photograph of Circulation Pattern (Solid Tracer, 3 minutes)	34
Figure 29	Mixing Time vs. Power/Unit Volume (Liquid Tracer) . .	37
Figure 30	Flow in Stack vs. Bubble Size	40
Figure 31	Mixing Time vs. Bubble Size	41
Figure 32	$\Theta\left(\frac{g}{D}\right)^{1/2}$ vs. $(Fr)^{1/2}\left(\frac{H}{D}\right)^{-0.20}$	44

Tables

		Page
I	Water Flow in Restricted System.	26
II	Percentage of Water Pumped During Mixing Operation	27
III	Efficiency of the Restricted System.	35
IV	Diffused Air Mixing of Large Bodies of Water	38
V	Effect of Disperser Submergence on Mixing Time	39

Conclusions

The conclusions given in this section refer only to the equipment and operating conditions used in this work.

(1) The mixing time, as experimentally determined, depends to some extent on the tracer technique used. Great care must be taken to ensure uniformity of the introduction of the tracer. Because of the randomness of the bubble motion, the circulation pattern undergoes random changes except for the well defined horizontal and surface jets. This randomness is responsible for the comparatively poor reproducibility of mixing time determinations.

(2) With air flow rates between 300 and 2000 cc/min, and volumes of water ranging from 100 to 180 gallons, the mixing time decreased slowly with increased air flow rate. However, below 300 cc/min a sharp increase in mixing time could be observed. It appears that decreasing the rate of flow a critical value is reached beyond which the currents generated are not sufficiently strong to establish a circulation of an appreciable magnitude in the whole body of water.

(3) The spread of experimental data increased with decrease of the air flow rate. The probable error of the mixing time determination increased from 8.6% at 2000 cc/min to 18% at 150 cc/min. Preliminary anemometric measurements of surface velocities in the vicinity of the plume indicated values ranging from 1 ft/sec at 2000 cc of air/min to 0.3 ft/sec at 150 cc/min. The velocity fluctuated between 25 to 50% with a tendency to increase at lower air flow rates.

(4) A good correlation was obtained between the mixing time and power input per unit volume of water. This correlation is of interest in scaling up model studies to large scale installations.

(5) Except for very low air rates (<150 cc/min) there was no apparent effect of water height on the mixing time. However, at the low air flow rate the mixing time was shorter at lower water heights. For two water depths the introduction of air at the side of the tank resulted in longer mixing times as compared with the central location of the disperser. The tests indicate that the central location of the plume gives a better mixing performance.

(6) Limited data was taken for two different depths of submergence of the disperser at the same air flow rate and water depth. The results showed that the smaller the energy input (smaller submergence) the longer was the mixing. It is emphasized that the greater is the distance between the disperser and the bottom of the tank the thicker is the comparatively stagnant bottom layer which hinders efficient mixing.

(7) Tests conducted with bubbles of different sizes showed that for bubble radii above the range of 0.06 to 0.12 cm the mixing time did not depend much on bubble sizes. However, below this range the velocity of rise of the bubbles, and therefore the density of the plume, dropped rapidly resulting in a shorter mixing time.

(8) The mixing time, the depth of water, and the principal dimension of the tank were successfully correlated by dimensional analysis with the densimetric Froude number. It is expected that still better correlation could be obtained with the use of a larger tank where the wall effect would be of smaller magnitude.

Recommendations

It is strongly recommended that the present research be continued in a tank of an approximate capacity of 5,000 gallons and at air flow rates of about 5 to 50 liters/min. The larger dimensions of the tank would allow a more accurate correlation of the variables. The experimental techniques as developed in the present work could be successfully applied without major modifications. The use of a larger tank would also allow a study of multiple air introductions which was impossible in the present work because of the small dimensions of the tank. The recommended investigation would thus constitute an intermediate step between the pilot scale studies as discussed in this report and the actual large scale investigation defined as Phase II in the original research proposal (WP-01376-01, Nov. 28, 1967, page 8).

SECTION I

Introduction

The storage of water in large lakes or reservoirs gives rise to problems of physical, chemical, and biological nature. Organic matter of industrial and natural origins tends to settle on the bottom where it decays, depleting the water of dissolved oxygen necessary to insure normal aquatic life. Although the upper surface of water which is in direct contact with the atmosphere may be saturated with oxygen, the mixing resulting from the density differences or the action of wind is usually too small to replenish the oxygen deficiency in the lower layers.

In order to alleviate these adverse conditions and improve the quality of water, attempts were made to destratify large bodies of water by artificial means of which the use of induced air seems to be one of the more promising.

A considerable amount of work has been conducted in the general field of circulation and destratification of large bodies of water by means of induced air (21). Little, however, has been published of a nature basic enough so that the results obtained in one case could be used to predict the results in another.

The objective of this work was to conduct a pilot scale study to estimate the effects of variables such as the air flow rate, geometry of the body of water, energy input, size of air bubbles, and the pumping capacity of the air plume on the time of mixing. The latter was defined as the time required to reach 90% of the equilibrium concentration of the KCl tracer. In studying the effects of the various variables, emphasis was put on their direction and relative magnitude in order to obtain better guidelines for large-scale investigation. It is expected that the rather successful correlation derived by dimensional analysis could be used as a starting point in correlating the results of large-scale tests.

The tests were conducted in a comparatively small tank (180 gallons) and therefore the obtained results should not be directly extrapolated to large bodies of water.

One of the main difficulties in conducting this kind of research is the pronounced randomness of the system caused by the random motion of bubbles. A great number of tests had to be conducted in order to obtain reliable averages.

Another difficulty was the unavailability of some of the measuring techniques. E.g. the determination of the velocity of rise of the air plume, required for the estimation of the density of the plume and therefore for estimation of the densimetric Froude number. Some of the techniques which have proved successful in one set of experimental

conditions gave erratic results when the conditions were changed.

A considerable part of this report will therefore be devoted to the description of the various experimental techniques and measurements even though some of them were later discarded as less reliable under conditions used in this work. They may, however, prove valuable under a different set of experimental conditions and therefore of interest to a future investigator.

It must be stressed that the induced air system was investigated only from the viewpoint of its mixing performance. Its effect on aquatic life was not considered in this work.

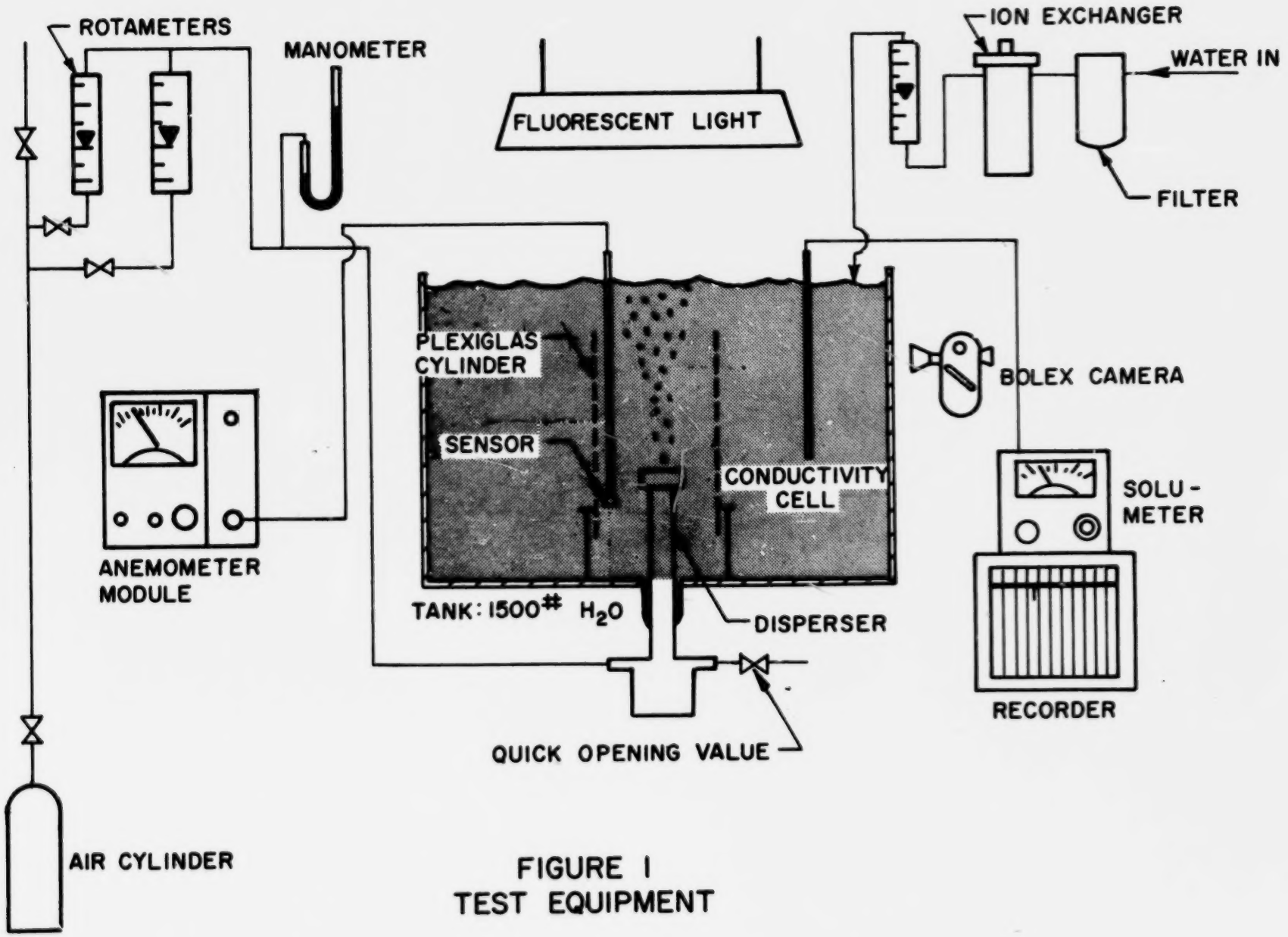

FIGURE I
TEST EQUIPMENT

BLANK PAGE

SECTION II

Equipment and Operational Procedures

General

The tests were conducted in a plexiglas tank (Figures 1 & 2) having a maximum capacity of 1500 lb. of water (180 gallons). The tank was rectangular in shape and was 48" long, 32" wide, and 36" high. It was mounted on a steel support with facilities for mounting auxiliary equipment and instruments. The plexiglas construction enabled photographic and motion picture investigation of the interior of the tank. In addition to the drain, the bottom of the tank had two openings for insertion of the air disperser. One of them was located in the center and the other 12" from the side and 15" from the front wall.

The water used in the tests was first passed through a porous filter to remove suspended matter and then purified in an ion exchange demineralizer. The specific resistance of this water was about 10^6 ohm-cm. The high resistivity water was necessary in the determination of the mixing time which involved the measurement of the changes of conductivity after introduction of the KCl tracer. The air to the disperser

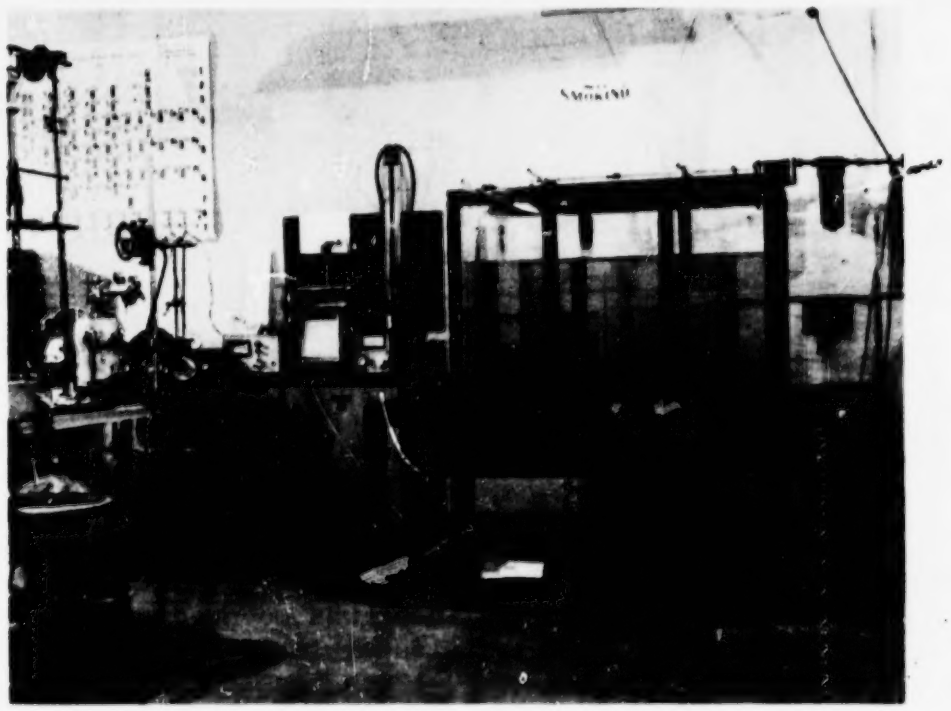

Photograph of Test Equipment
Figure 2

PRECEDING PAGE BLANK

was supplied from a breathing air cylinder and metered by two rotameters. The air disperser consisted of an Aloxite plate, one inch in diameter, cemented in a brass holder. The height of the holder could be adjusted to vary the depth of submergence of the disperser.

The Restricted System (Figure 3)

The air plume issuing from the disperser undergoes a random swaying motion during its rise to the surface. This lack of stability affects the dimensions of the plume, the water flow pattern, and makes difficult the anemometric measurement of the water flow produced by the plume.

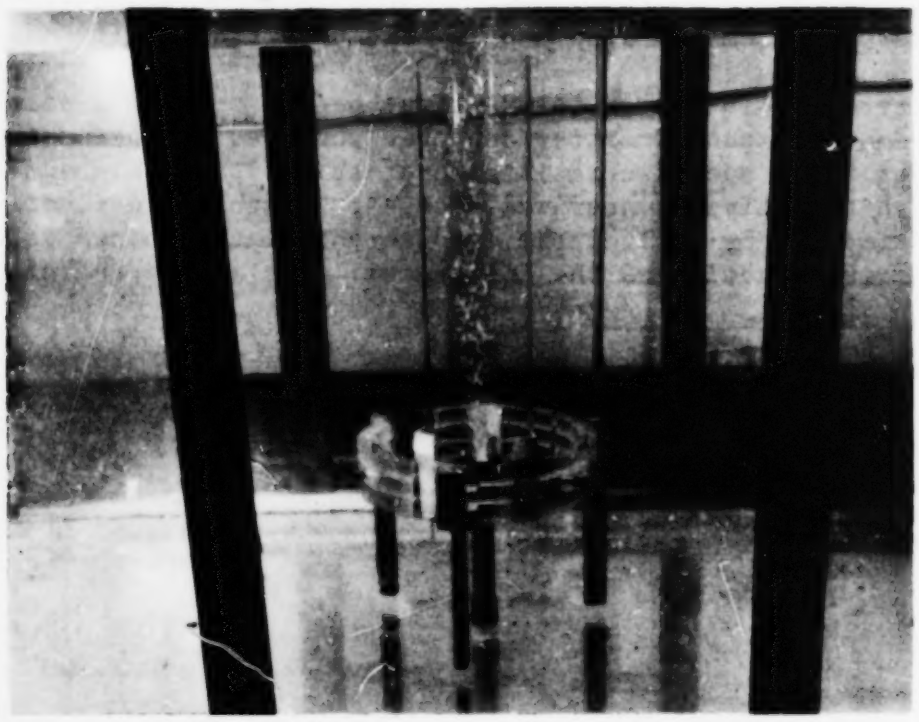

Photograph of Restricted System
Figure 3

In order to decrease this difficulty, and to improve the reproducibility of the water flow measurements, some tests were conducted in a system in which a plexiglas cylinder was mounted around the plume. In a later part of the report this cylinder is referred to as stack. The cylinder was 4 inches in diameter, 18 inches long, and its lower end was at a distance of 4 inches from the bottom of the tank. The upper end was 2 inches below the level of water. Although the presence of this cylinder increased somewhat the flow resistance of the system, it enabled at the same time to obtain valuable data on the pumping performance of the plume. It is of interest to note that under identical operating conditions the mixing timesobtained with and without the cylinder were practically the same. The above indicates that the

presence of the cylinder did not exert any major effect on the operating efficiency of the system despite the fact that the flow pattern in the vicinity of the plume was changed. In the freely rising plume the surrounding water entered the plume through its sides up to the level just below the surfact jet. In the restricted system this side inflow was eliminated by the presence of the cylinder and the water was forced to flow at a uniform rate from the bottom to the top of the cylinder.

Determination of the Bubble Size

Since the pumping action of the plume depends on its buoyancy and therefore on the density of the air-water dispersion, it was decided to investigate the effect of the size of the bubbles. It was expected that the decrease in the size of the bubbles and the resulting drop in the velocity of rise would increase the air-holdup, decrease the density of the plume and thus improve the pumping effect. It appears from our literature survey that very little information is available in this field.

The bubble size was determined in this work by photographing the bubbles rising in the air plume. A Bolex 16 mm movie camera with a telephoto lens and Kodak 4X negative film were used in this determination. The lighting was accomplished by a 1531-A Strobotac and 1539-A Stroboslave (G.R.C.). The lamp of the Stroboslave was placed in the back of the tank and the flash was directed through the tank into the lens of the camera. A white paper backing was used at the back of the tank to reduce intensity of the flash. A metal rod of known diameter was used as a standard of reference. It was mounted at an angle to the camera so that a part of it was always in focus. Pictures obtained by this back lighting technique were of excellent contrast (See Figure 4). After developing, the film was projected and the major and minor axes of at least 40 bubbles were measured and the equivalent spherical radius was calculated for each bubble. The average equivalent spherical radius was then used in evaluation of results. The accuracy of this method was checked by means of glass spheres of known diameters and was found to be $\pm$ 1.5%.

Since the photographs taken at the bottom of the plume and at its top showed practically the same bubble sizes and distribution, the bubbles were photographed only at the top of the plume.

The uniformity of bubble sizes was very satisfactory at air flows of 500 cc/min S.T.P. and higher. At lower flows, however, the uniformity of sizes decreased resulting in a greater error of measurement. To obtain a conservative estimate of the reproducibility of the measurement, the probable error was estimated at the low flow rate of 300 cc/min S.T.P. and was found to be 6.2%.

Photograph of Air Bubbles
Figure 4

Photograph of Air Plume
Figure 5

Determination of the Shape of the Air Plume

The shape of the air plume is necessary for the determination of the plume density required in the densimetric Froude number. The measurements of the plume were taken by photographing the plume and a reference scale by means of a Polaroid MP-3 camera. The black and white photographs were projected and the diameters were measured at various heights of the plume (See Figure 5). The impression that the bubbles did not reach the surface of the water was caused by the tilt of the camera when taking this particular photograph. At first the pictures were taken from both sides of the tank to estimate the possible effect of the different plume to wall distances. Since no difference was observed, only one side of the plume was photographed and in the calculations the plume was assumed to be a perfect cone.

For rates of air flow below 2000 cc/min S.T.P. the plume was very stable. However, at higher flow rates the plume became unstable due to horizontal swaying. On two occasions the bubbles in the plume formed a vortex. The volume of the plume was calculated by the equation:

$$V = \left(\frac{\pi H}{3}\right)\left(r_1^2 + r_1 r_2 + r_2^2\right)$$

where V = volume, cc.

H = depth of immersion of disperser, cm.

r_1 = radius at plume top, cm.

r_2 = radius at plume bottom, cm.

From the known volume of the plume and the instantaneous volume of air (air holdup), the plume density can be easily calculated from the relationship:

$$\rho_w = \frac{(V - v)\rho_w + v\rho_a}{V}$$

where: v = instantaneous volume of air, cc.

ρ_w = density of water, g/cc.

ρ_a = " of air, g/cc.

The Velocity of Rise of the Plume

The velocity of rise of the plume is an important quantity for the determination of the instantaneous volume of air (air holdup) necessary for estimation of the density of the plume. The principle of this measurement is based on creating a disturbance in the plume and following this disturbance by means of motion picture photography.

The disturbance was produced by an abrupt discontinuation of the air flow by means of a quick release valve which vented the air into the atmosphere (See Figure 6).

The vertical displacement was determined with the help of a reference scale mounted parallel to the plume. The corresponding time was obtained from the number of frames and the known framing rate of the Bolex movie camera.

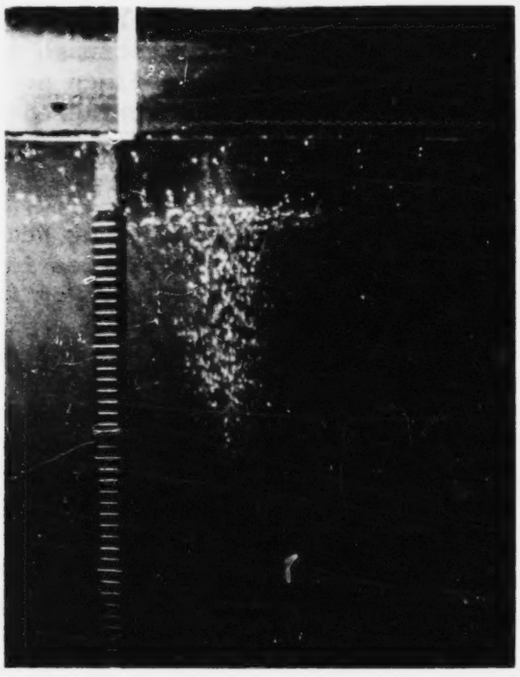

Photograph of the Rising Disturbance of the Plume
Figure 6

For each run 5 or 6 determinations were made and the results averaged. The framing rate of the camera was checked by photographing the dial of a milli-second timer and counting the number of frames for a set time. This method of velocity determination was subject to two errors. At low air velocities (below 600 cc/min) the line of disturbance started to become irregular because of increasing irregularity in the size of the bubbles and, therefore in their velocity of rise. This problem did not occur at higher air flow rates. The other difficulty was caused by the effect of the disturbance on the velocity of circulation in the tank. In order to decrease this effect, the velocity of rise was measured up to a distance of 8 to 10 inches above the disperser. In this way, the air flow was interrupted for only about one second. To check this technique a hot film anemometer was mounted within the plume and the water velocity was measured after the interruption of the air flow. The measurement showed that the water velocity remained constant for approximately 1 second within the region used in our measurements.

The instantaneous air volume "v" (air holdup) in the tank was calculated from the equation:

$$v = (H/v_r)Q$$

where: H = depth of immersion of disperser

Q = air flow rate

v_r = velocity of rise of plume

Measurement of the Water Flow in the Tank

The rate of water flow produced by the air plume was measured by means of hot film anemometry. A cylindrical hot film sensor (TSI Model 1210 60W) and the anemometer module (TSI Model 1053-B) were used in this work. The constant temperature anemometer measured the fluid velocity by sensing the rate of heat transfer from the heated sensor to the surrounding water which was kept at constant temperature. As the water velocity increased, the sensor tended to cool, changing the resistance. The amplifier then adjusted the current to the sensor to maintain constant temperature. These changes in the output of the amplifier were then related to changes in water velocity by means of calibration.

The use of anemometer in this work was not without errors. Lint or other suspended impurities could have collected on the sensor, producing change of heat transfer unrelated to the change in water velocity. Formation of minute air bubbles on the wire of the anemometer was another potential source of error. In order to detect bubble formation, the sensor was illuminated by a beam of light and observed with a magnifying glass. Usually a light knock on the sensor holder would displace the bubble. Decrease of the sensor temperature by lowering the current was of help in decreasing bubble formation but at the same time adversely affected the sensitivity of the instrument.

The sensors were calibrated in a TSI Model 1125 Calibrator. A cross-section through the calibrator nozzle and the sensor is shown in Figure 7. The sensor wire (invisible on the photograph) is in the center of the nozzle supported by the V-shaped arms of the probe. In order to avoid breaking of the delicate and expensive sensor, a special protecting device was constructed (see upper part of the Figure) which prevented damage to the sensor while inserting and removing it from the calibrator. The flow of water through the instrument was measured by a calibrated rotameter. Addition of dye showed a flat velocity profile at the plane of the sensor. To insure against changes in calibration each probe was calibrated before and after each test.

Initially it was proposed to determine the pumping effect of the air plume from the velocity profile of the surface jet (Figure 8). Unfortunately, the randomness and turbulence of flow in the surface jet

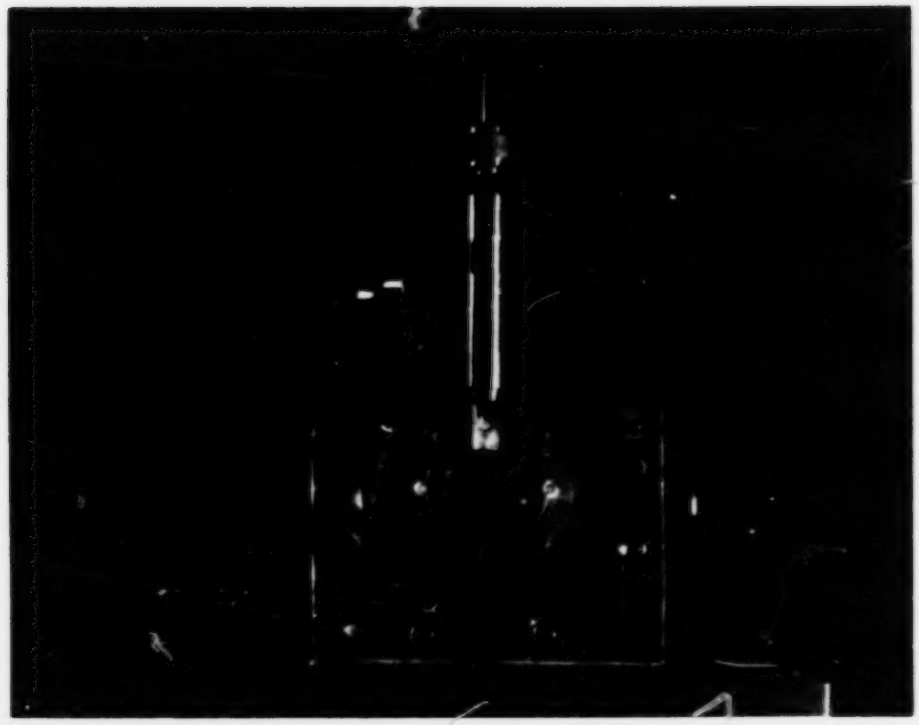

Photograph of Anemometer in Calibrator
Figure 7

gave erratic results. Consequently, no attempt was made to measure the velocity profiles in this region. The measurement of the water velocity was therefore limited to the restricted system where the velocity was measured in the cylinder at a level below the disperser.

A photographic technique for measuring the flow of water was also briefly investigated. Selected polystyrene beads (Comak Chemicals Ltd., London, N.E. England) of density close to that of water were allowed to circulate in the tank. The beads were photographed by means of the Polaroid MP-3 camera and stroboscopic illumination. Every time the stroboscope flashed an image of the bead appeared on the film (Figure 9). From the distance between the images and the known rate of flashing, the velocity component in the vertical direction was calculated. Usually a few pictures were taken and the average velocity was calculated. The difference between the anemometer and photographic measurements was in the range of 10 to 15%.

The anemometric technique was selected in this work because of its simplicity and the fact that it can be used for measurement of point velocities.

Determination of the Mixing Time

The mixing time is one of the most important quantities studied in

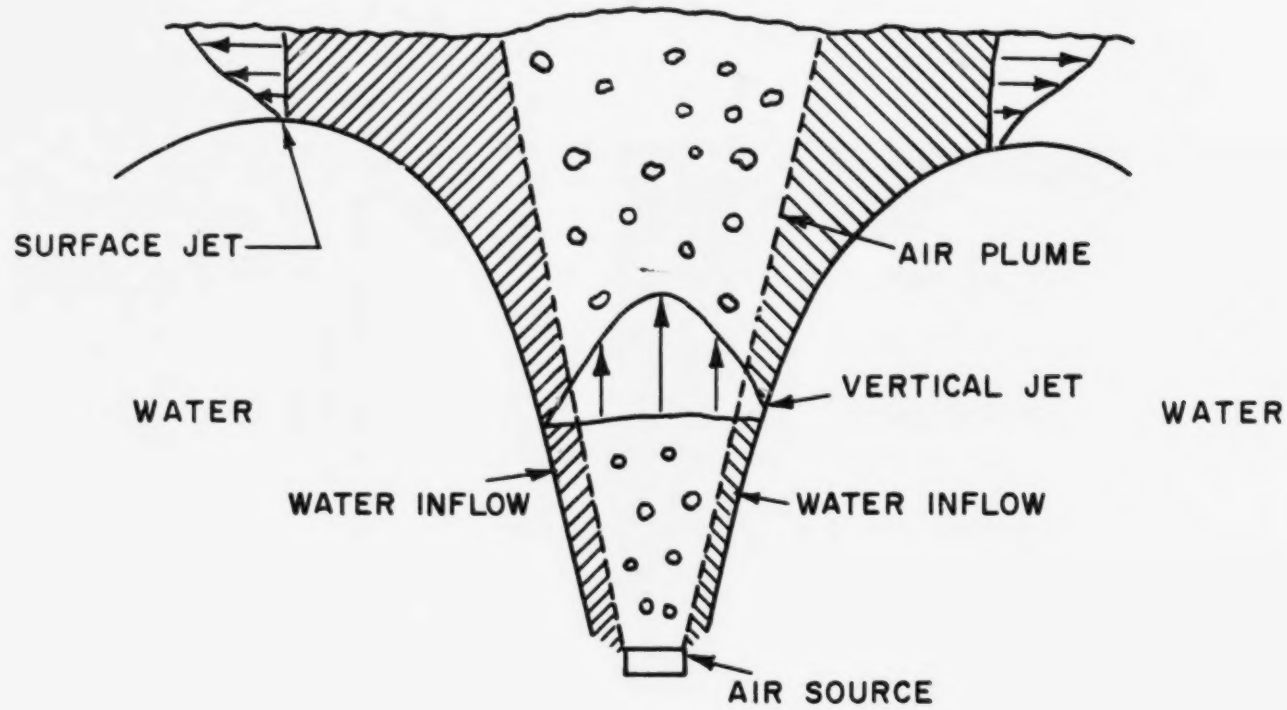

FIGURE 8

PUMPING ACTION OF PLUME

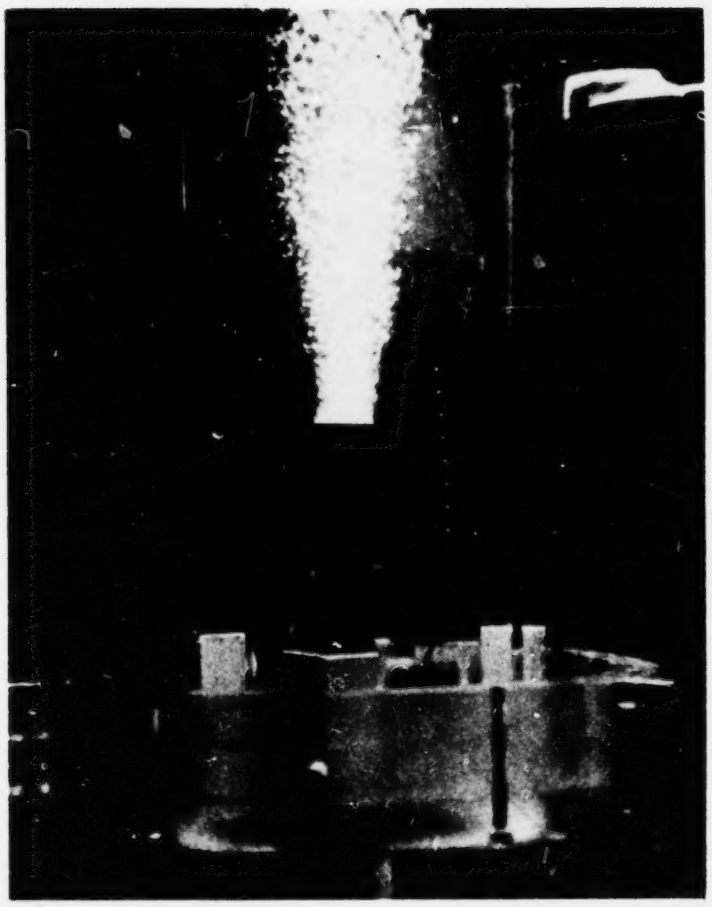

Photograph of Water Velocity Determination by Stroboscopic Photography
Figure 9

this work. Considerable time was spent on developing of various techniques and on estimation of their relative merits. The principal difficulty of this measurement lies in the randomness and poor reproducibility of the system itself. The randomness of bubble motion is mostly responsible for it. It is therefore practically impossible to find out to what extent this poor reproducibility is due to the method of determination.

Gay and Hagedorn (5) in their study of mixing of stratified bodies of water measured changes in salinity. Similarly Harrell (7) used changes in conductivity in his flow of fluid system. Zlokarnik (24) estimated the mixing time by adding acid to a solution of a base in the presence of phenolphthalein and following the change of color. Nickerson (14) introduced a fluorescent dye, Rhodamine, into a water reservoir and monitored the changes with a fluorometer. In other investigations (16) changes in temperature and oxygen concentration profiles were used to advantage.

In the methods applied in this work the mixing time was estimated by introducing a KCl tracer and following the changes in conductivity. A Beckman Solu-Meter (Model RA-5) with temperature compensation and Leeds & Northrup Speedomax recorder were used in the investigation. The cells were Epoxy Dip Type fabricated from 5/16" diameter epoxy rod 2 ft. long and having unshielded platinized nickel electrodes of 0.2/cm cell constant.

Three different tracer techniques were investigated. In the first method 200 cc of KCl solution was introduced at the surface through a 1/8 inch opening. The concentration of the solution was so selected as to give a conductivity change of 20 micromhos. At this conductivity change one full tank of water could have been used for 8 tests.

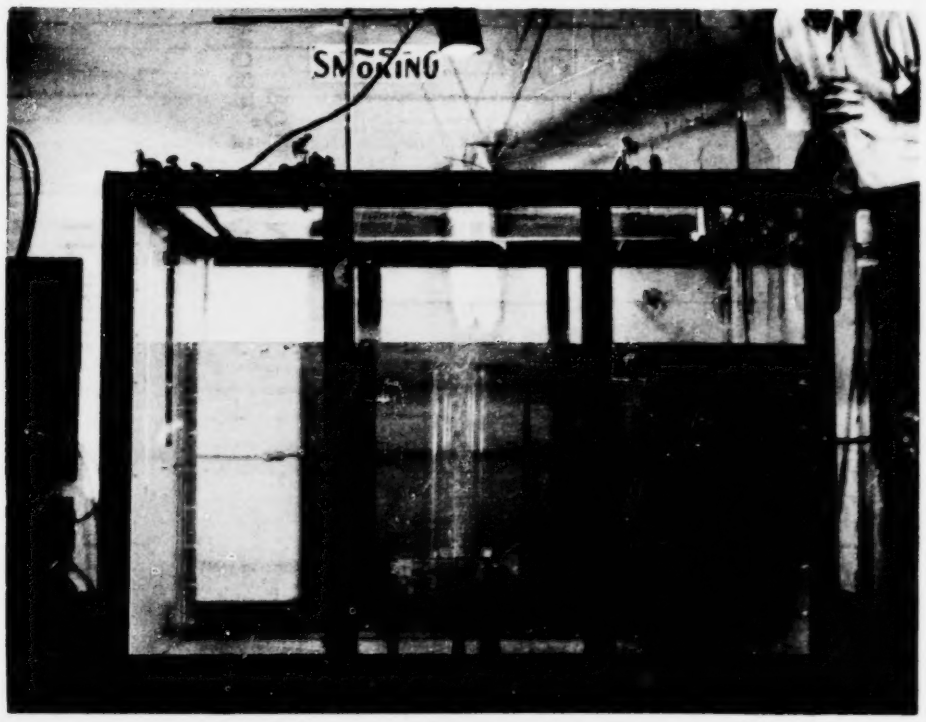

Photograph of Liquid Tracer Introduction
Figure 10

Figure 10 shows a black dye being introduced by this technique. The tube was located 2 inches from the right side wall. The conductivity cells were placed on the opposite side of the tank in several locations (See Figure 11).

Before each test the air flow was adjusted to the required value and allowed to flow through the tank for at least 30 minutes before introduction of the tracer. This was necessary to establish a uniform flow pattern and avoid temperature gradients in the tank which would affect the conductivity measurements. At the end of the test when the conductivity approached equilibrium value, the contents of the tank

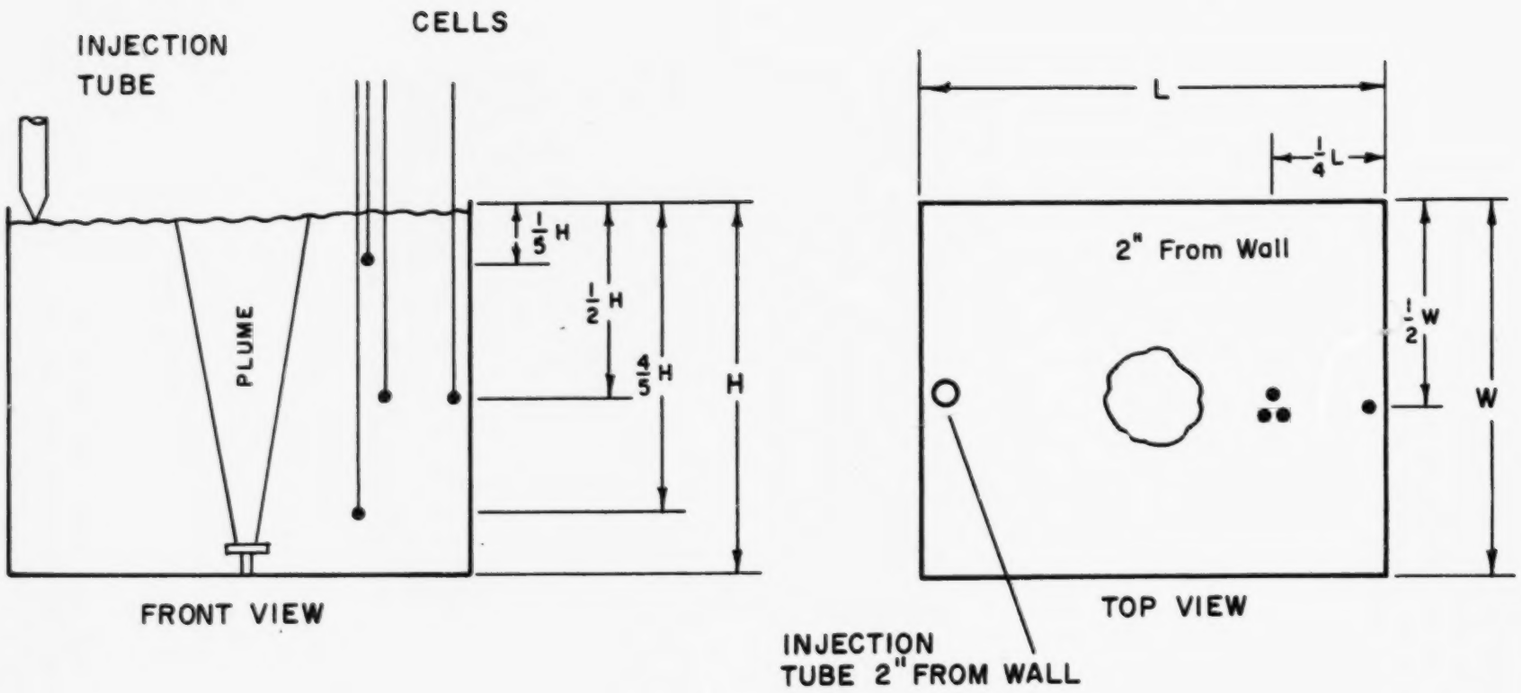

FIGURE 11

CONDUCTIVITY CELL LOCATIONS

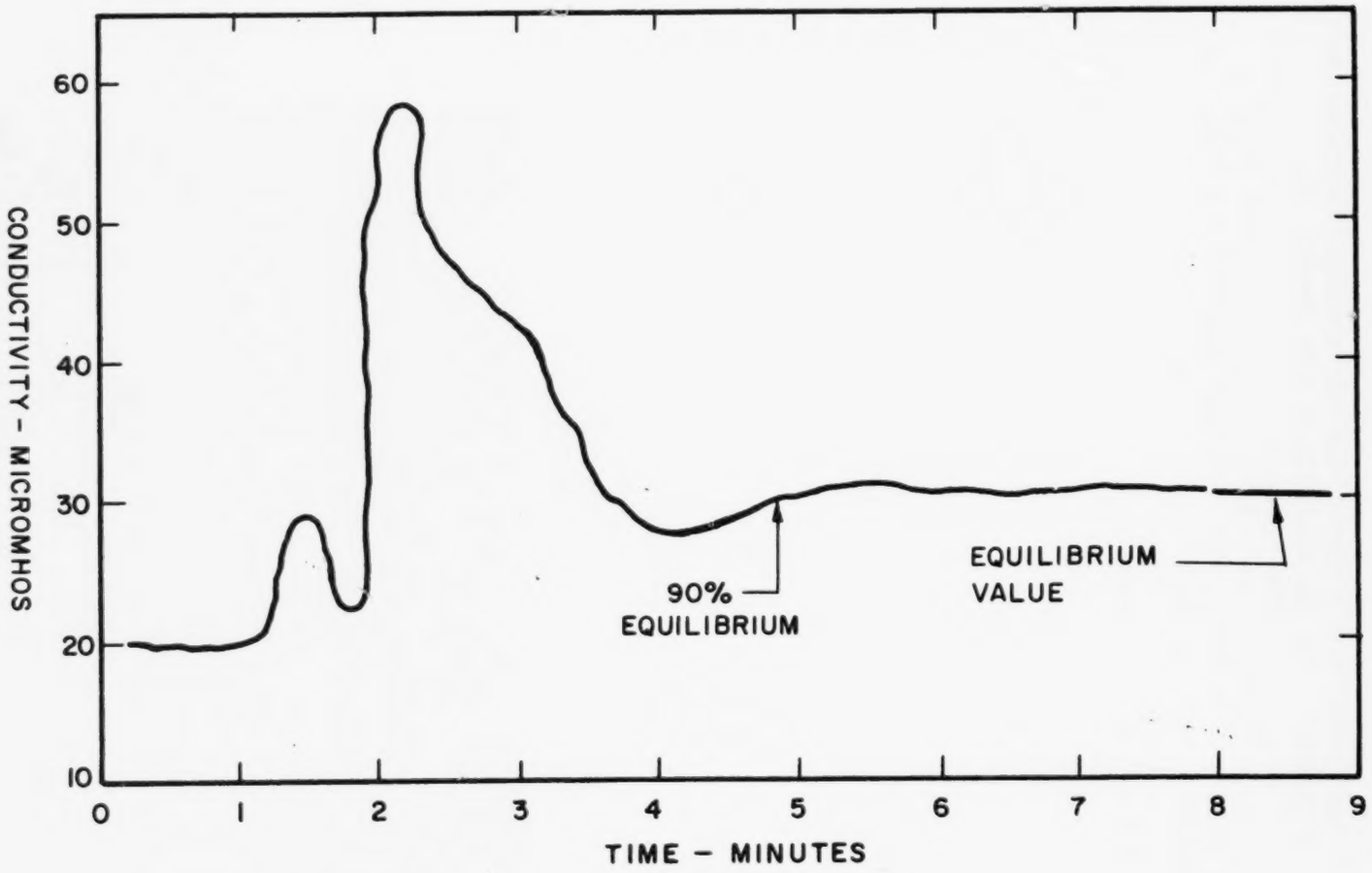

FIGURE 12

CONDUCTIVITY VS TIME CHART (SOLUTION TRACER INTRODUCTION)

were vigorously mixed with a paddle and the terminal (equilibrium) conductivity determined. In the analysis of the charts, the time corresponding to 90% of the terminal conductivity was arbitrarily selected as the mixing time. A representative sample of a recorder chart is shown in Figure 12 where the horizontal axis was reduced by a factor of two and the vertical axis was expanded by the same factor.

For each set of experimental conditions a total of eight tests were conducted (2 tests for each cell location) and the results averaged. A series of photographs showing the progress of tracer distribution will be shown in the section dealing with the interpretation of results.

A number of tests conducted under analogous experimental conditions showed a probable error of a single determination to be 8.6% and 18% at the air flow of 2000 and 150 cc of air/min respectively. As was mentioned before, this value reflects also on the effect of the randomness of the system.

In the second tracer technique, ground KCl crystals were spread over the top of the air plume. The crystals were ground to a fine powder to ensure their dissolution before reaching the bottom of the tank. They were spread uniformly by means of a perforated dish over a circular surface, 5 inches in diameter. A metal ring of this diameter was placed above the top of the plume to insure a uniform and more reproducible addition of the tracer. Figure 13 shows a dye being introduced by this technique. The conductivity cells were placed in

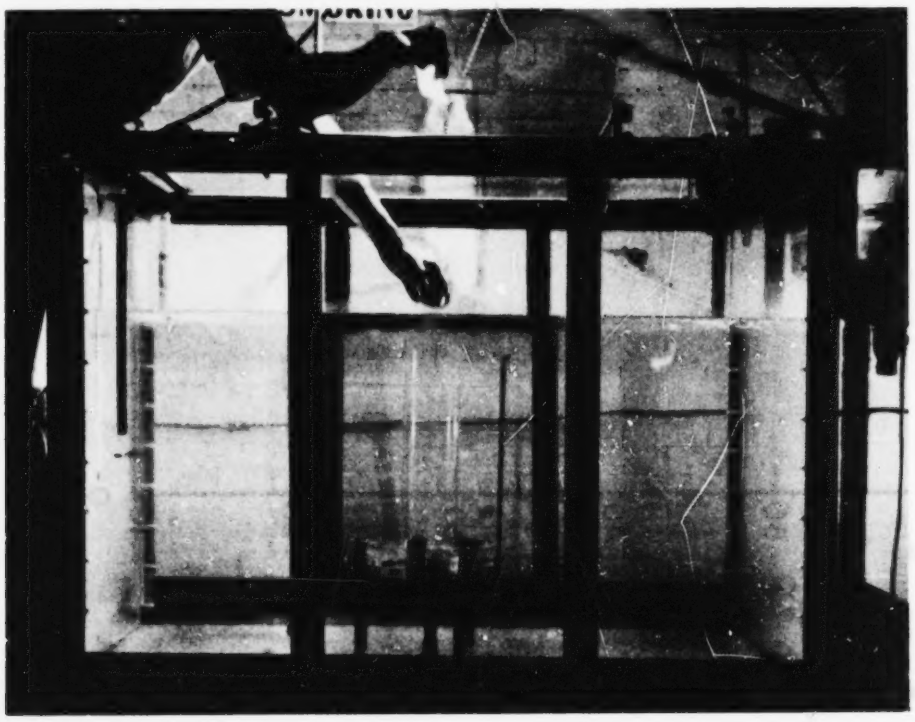

Photograph of Solid Tracer Introduction
Figure 13

geometric centers of each half of the tank. The conductivity versus time data were obtained by switching from one cell to the other every 10 seconds. In the analysis of the chart the two conductivity readings were averaged and plotted against time (See Sigure 14). The mixing time was defined as that point at which the average conductivity was $\pm$ 5% of the terminal (equilibrium) value. The average value of the 2 cells was used because there was always some tendency of the crystals to be carried more to one side than to the other. The probable error of this measurement was found to be 9.2%. As in the first method the effect of the randomness of the system is included in this figure.

The third method investigated in this work consisted of adding a dilute KCl solution at a constant rate over a period of 30 minutes. It was expected that in this way the effect of the randomness of the flow pattern on the mixing time would be decreased. Again as in previous methods enough salt was added to produce in the mass of water a change in conductivity of 20 micromhos. If the mixing time were zero (instantaneous mixing), the conductivity vs. time curve (line A Figure 15) would form a straight line starting from the origin. However, since the mixing is never instantaneous, the actual curve is displaced by the amount corresponding to the time required for mixing. This method has an unquestionable advantage over the previous techniques in the fact that the time of tracer introduction was much longer and therefore the effect of the randomness of the system considerably decreased. This method was not used in our work because of the lengthy analysis of the charts.

On the whole it may be said that the estimation of mixing times from conductivity measurements was experimentally simple. It had, however, the disadvantage of the use of large quantities of low conductivity water and therefore the necessity of frequent (each 6 to 8 tests) exchange of the contents of the tank.

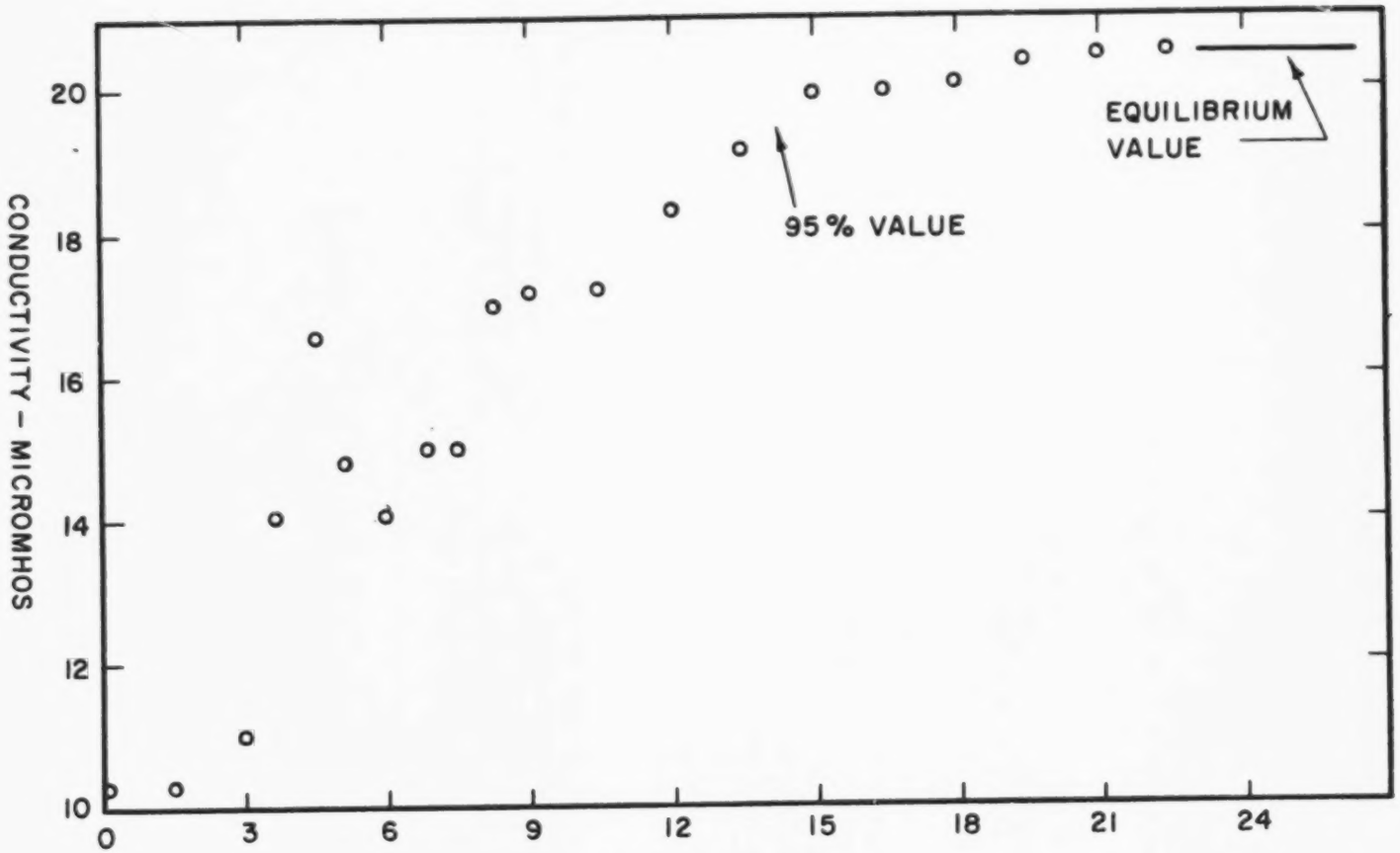

FIGURE 14

CONDUCTIVITY VS TIME (SOLID TRACER INTRODUCTION)

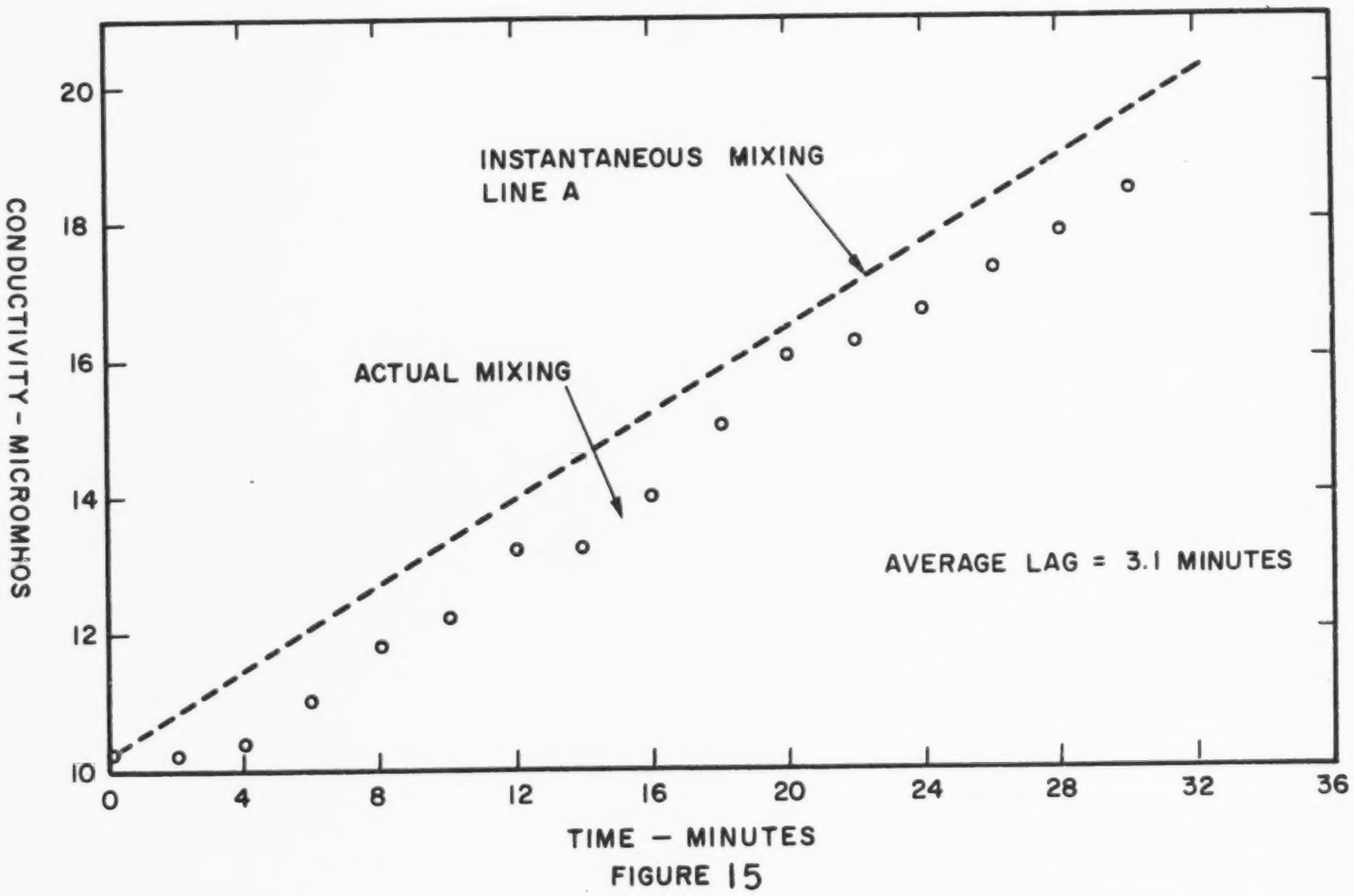

FIGURE 15

CONDUCTIVITY VS TIME (CONTINUOUS TRACER INTRODUCTION)

BLANK PAGE

Section III

Discussion of Results

The Effect of Air Flow Rate on the Mixing Time.

The results of this group of tests are summarized in Figures 16 and 17. In Figure 16 the height of the water in the tank was used as a parameter while Figure 17 also shows the effect of the location of the air disperser. It must be noted that in Figure 16 the branch of the curve between air flows of 300 to 2000 cc/min is an average of the three water heights (15, 24, 30 inches) investigated in this work. This was done because in this region the water heights studied did not show a definite effect on the mixing time. In the region of air flows below 300 cc/min. curve A represents the average of the data taken at 24 and 30 inches of water while curve B represents the average for 15 inches. In Figure 16 the liquid tracer was used while in the tests presented in Figure 17 solid tracer was introduced over the plume for estimation of mixing times. The curves, therefore, are not directly comparable.

In both figures the bubble sizes (equivalent spherical radius) varied from 0.07 cm at 150 cc/min to 0.18 cm at 2000 cc/min of air. It will be shown later that the effect of this difference in bubble sizes on the mixing time is negligible. The effect of geometry (water height and disperser location) will be discussed in a separate section of the report.

It can be seen from both figures that the mixing time becomes shorter with increase of the air flow rate. This dependence, however, becomes less pronounced at higher rates of flow. As was mentioned before, the mixing time, as measured in this work, is influenced by the randomness of the system, as well as by the details of the tracer technique. It seems therefore advisable to discuss first the circulation currents established in the tank as a result of the pumping action of the air plume.

The water entering the plume is pumped upwards because the potential energy of the rising bubbles is transformed into the kinetic energy of the water (1, 11, 13). In the forthcoming discussion this water current will be referred to as the vertical jet (Figure 8). Upon reaching the surface the bubbles escape into the atmosphere but the momentum of the vertical jet is converted into a thin horizontal surface jet (1, 10, 18). According to Baines (1) the thickness of this current is less than 5% of the depth of the submergence of the disperser. It can be seen from Figure 13 that this surface jet is very thin.

PRECEDING PAGE BLANK

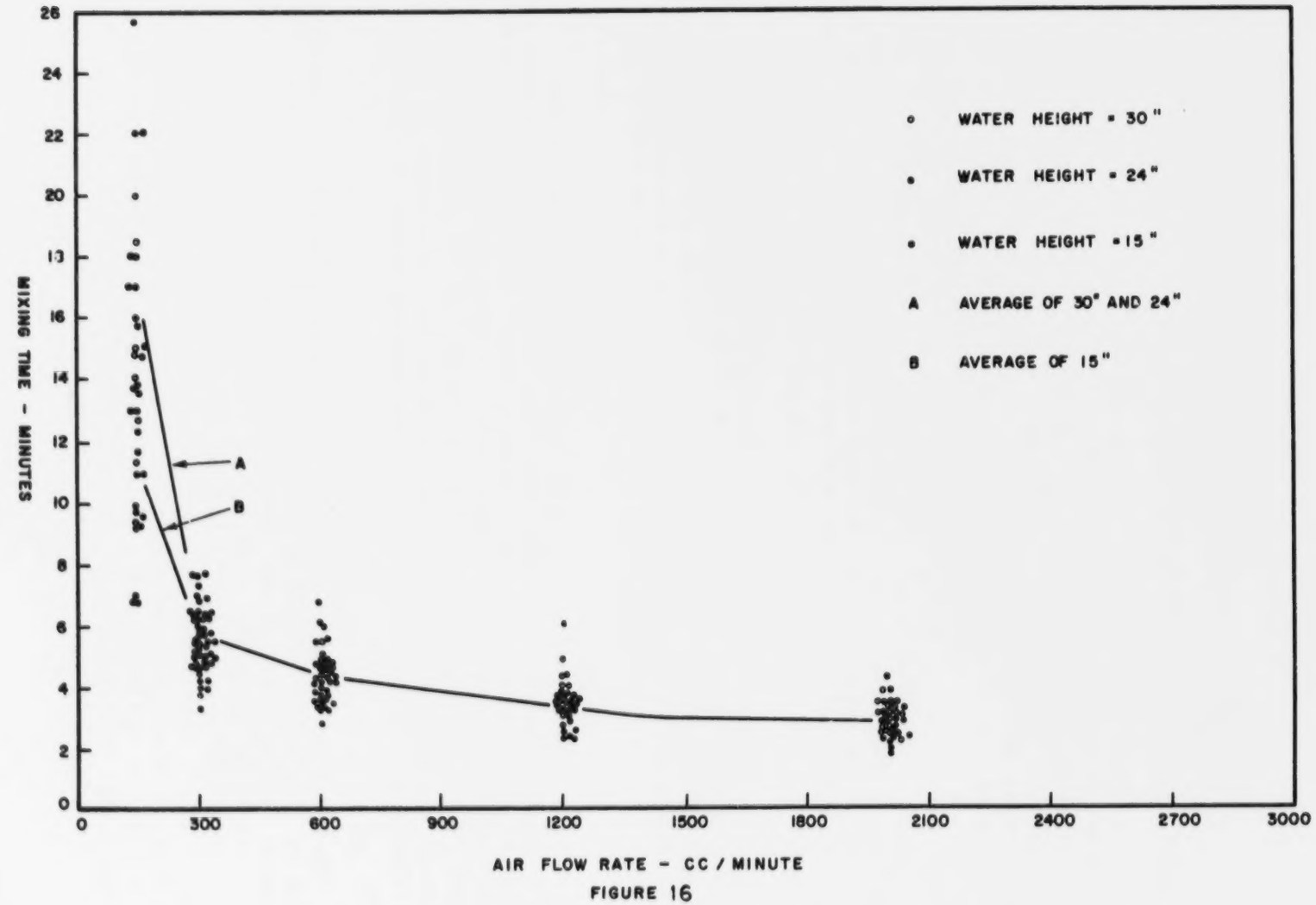

FIGURE 16

MIXING TIME VS AIR RATE (LIQUID TRACER INTRODUCTION)

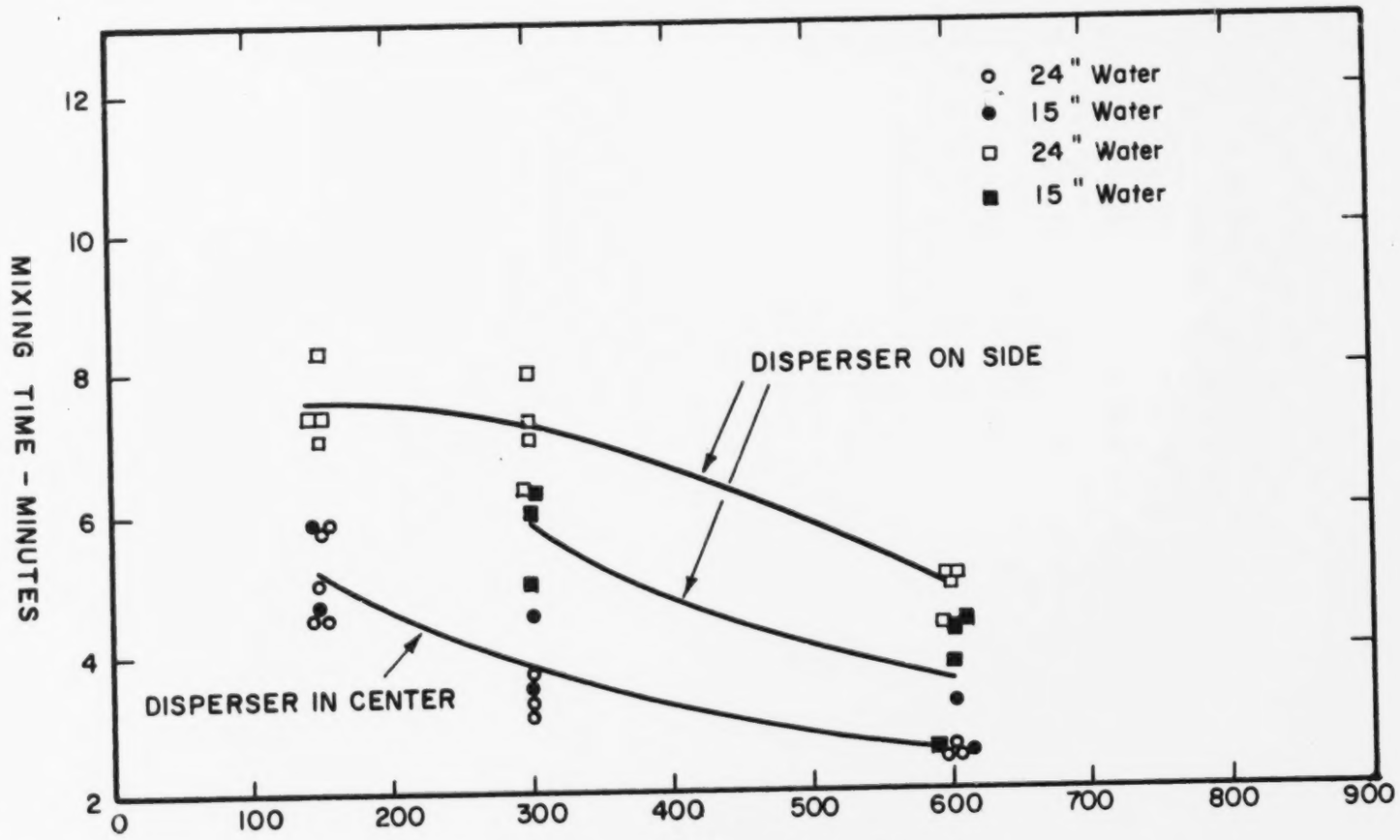

FIGURE 17

MIXING TIME VS AIR FLOW RATE (SOLID TRACER INTRODUCTION)

This surface current produced by the vertical jet has been studied by a number of investigators (1, 4, 10, 18, 19). Most of them (4, 10, 18, 19) were interested in its damping action on ocean waves (pneumatic breakwaters). They found that the water velocity of the surface jet was inversely proportional to the distance from the plume. Hence, the momentum of the surface jet was used to generate currents in the layers below.

Gay and Hagedorn (5) studying induced air mixing of a stratified body of water found in addition to the surface jet a strong bottom current toward the disperser and a stagnant zone in the vicinity of the disperser. The presence of this stagnant layer was also noticed by Straub et al. (18) in their work on pneumatic breakwaters. It is also of interest to note that the presence of this zone may constitute a potential source of error in mixing time determination. Figures 24 to 28 give a good idea of the water circulation pattern encountered in the present work.

The effect of the air flow rate on the water flow (and therefore on the mixing time) can best be seen in Figure 23 where the restricted system was used and the water velocity was measured directly by hot film anemometry. The results shown in this figure were taken at a constant water height. The form of this curve is in agreement with the data of Kurihara (10) obtained in an unrestricted system. He found that the flow of water is proportional to the air-flow rate to the 1/3 power.

Table I gives the values of $\frac{F}{Q^{1/3}}$ calculated from Figure 23. It can be seen that except for the lowest rate of air the above relationship between the flow of water (F) and that of air (Q) applies well to the system investigated in this work.

Table I

Water Flow in Restricted System

Flow of Water (F) liters/min	Air Flow (Q) cc/min	$\frac{F}{Q^{1/3}}$
10	50	2.7
20	110	4.2
30	225	4.9
40	500	4.9
50	1050	4.9

This interdependence was also confirmed by Cyr (3) for higher air flow rates. Taylor (19), in fact, showed theoretically that the maximum vertical current of water produced by a flow of gas is proportional to the 1/3 power of the gas flow rate. Table II shows the dependence of the mixing time on the water pumped in the restricted system. The mixing times were determined by the solid tracer technique.

Table II
Percentage of Water Pumped During Mixing Operation

Air Flow cc/min	Mixing Time Minutes	Total Water Pumped in Mixing Time, Liters	% Tank Capacity Pumped
150	8.34	200	33
300	4.92	170	28
600	4.11	175	29

Water volume = 610 liters

The table shows a close dependence of the mixing time on the amount of the water pumped. It is of interest to note that only about 30% of the tank capacity had to be pumped in order to approach closely the equilibrium concentration.

Bryan (25) states that in the diffused air mixing of the Blellam Tarn reservoir only 26% of its volume was pumped during the time required for mixing. Although the reservoir may not have been as well mixed as the tank used in this research, this information does serve to illustrate the importance of the currents generated by air dispersion.

It was already stressed before that Figures 16 and 17 differ in the method of tracer introduction. In the former, liquid tracer was introduced close to the smaller wall of the tank, while in the latter the solid tracer was added over the top of the plume. On the whole it may be said that the liquid tracer introduction (Figure 16) showed greater mixing time than the corresponding curve for solid tracer (Figure 17, disperser in center). This difference in results was probably due to the fact that in the case of liquid tracer, the whole volume of the solution was introduced in a pulse which spread into the region of comparatively stagnant liquid at a considerable distance from the plume. On the other hand, the solid tracer was added in the center of the surface jet where the chance of its rapid distribution was much better.

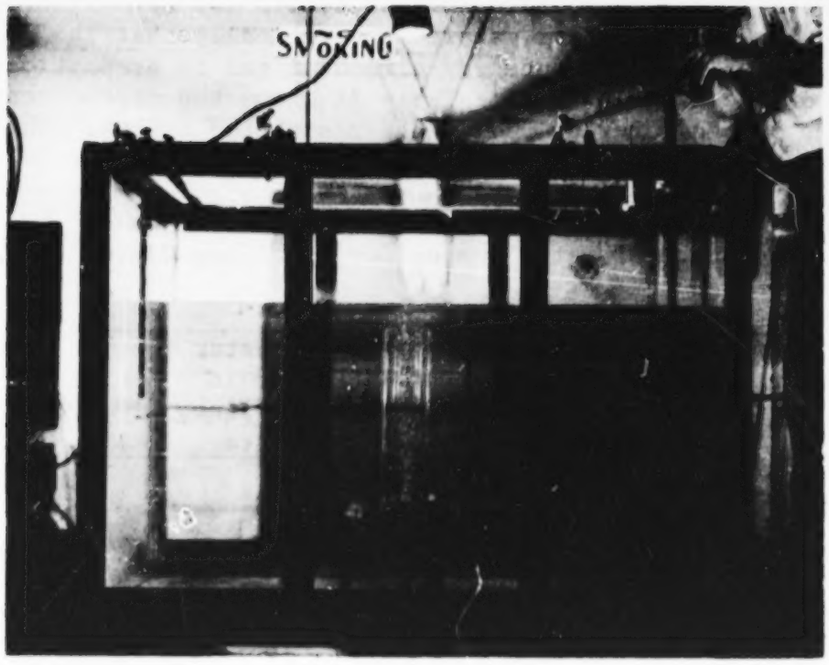

Photograph of Circulation Pattern; 10 seconds. Solution Tracer
Figure 18

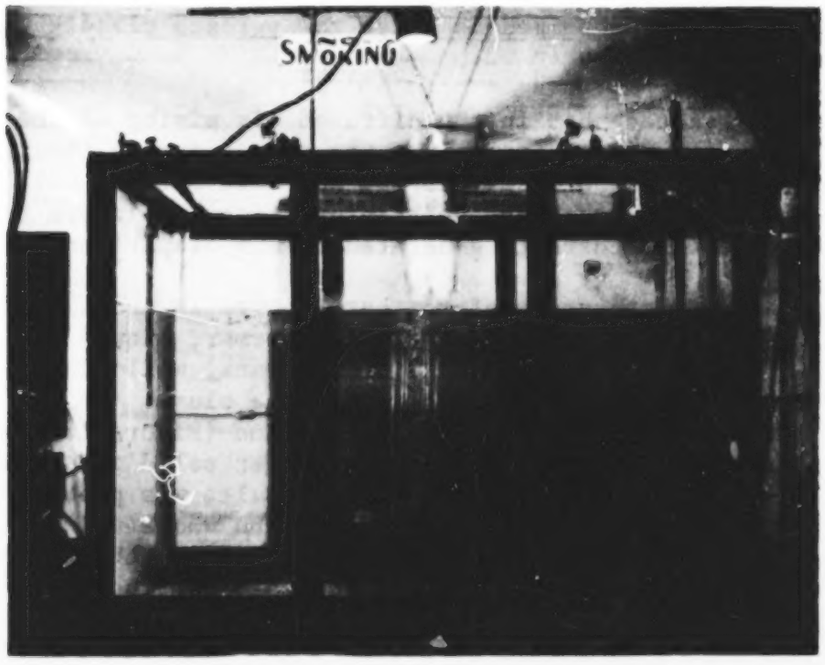

Photograph of Circulation Pattern; 30 seconds. Solution Tracer
Figure 19

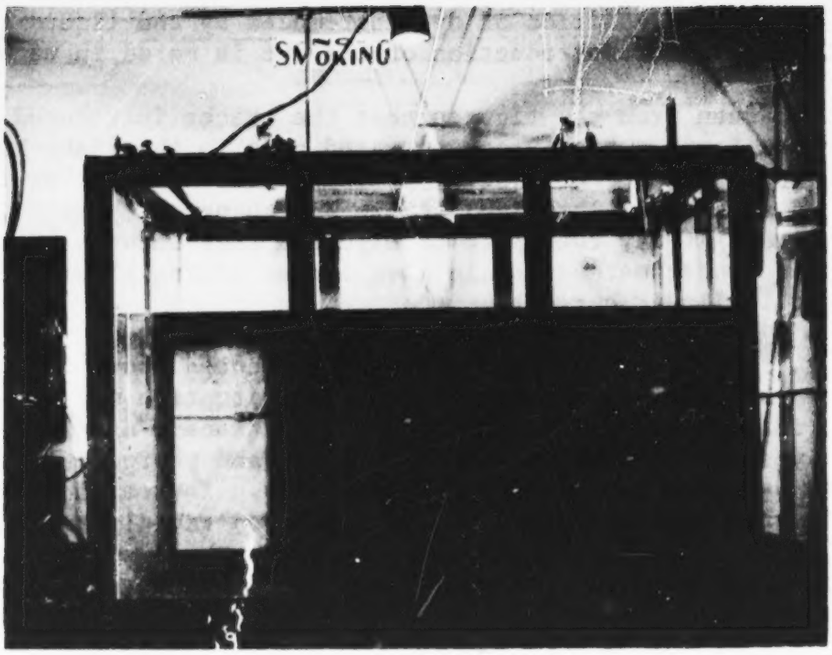

Photograph of Circulation Pattern; 1 minute Photograph of Solution Tracer
Figure 20

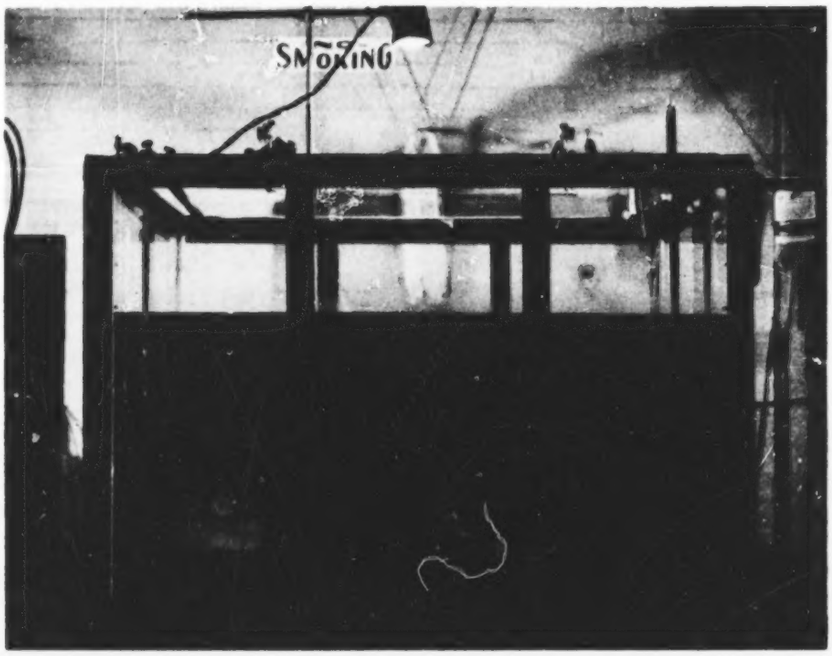

Photograph of Circulation Pattern. 2 minutes Solution Tracer
Figure 21

Figures 18 to 22 show addition of dye introduced by the liquid tracer method. The time after introduction of the dye is noted in each Figure.

It can be seen from the figures that the tracer introduced in the form of a pulse forms a highly concentrated zone in the right-hand side of the tank which has to be "pulled" by the slowly circulating liquid to the left-hand side (cell location) before any changes in the conductivity can be detected. It may therefore be expected that because of this initial lag the liquid tracer method should give longer mixing times as shown in Figure 16 and 17 (lower curve).

However, in the case of solid tracer introcuced above the plume, that is in the center of the surface jet, the situation was different. In order to illustrate the distribution of the tracer, a small quantity of a black dye was mixed with the KCl crystals and photographs were taken at time intervals between 10 sec. and 3 minutes. The results are shown in Figures 24 to 28. The tiny crystals dissolved rapidly and the resulting solution was spread uniformly over the whole surface of the tank. This, already dilute solution, was then distributed throughout the mass of water by the circulation currents produced by the plume.

Photograph of Circulation Pattern. 3 minutes Solution Tracer
Figure 22

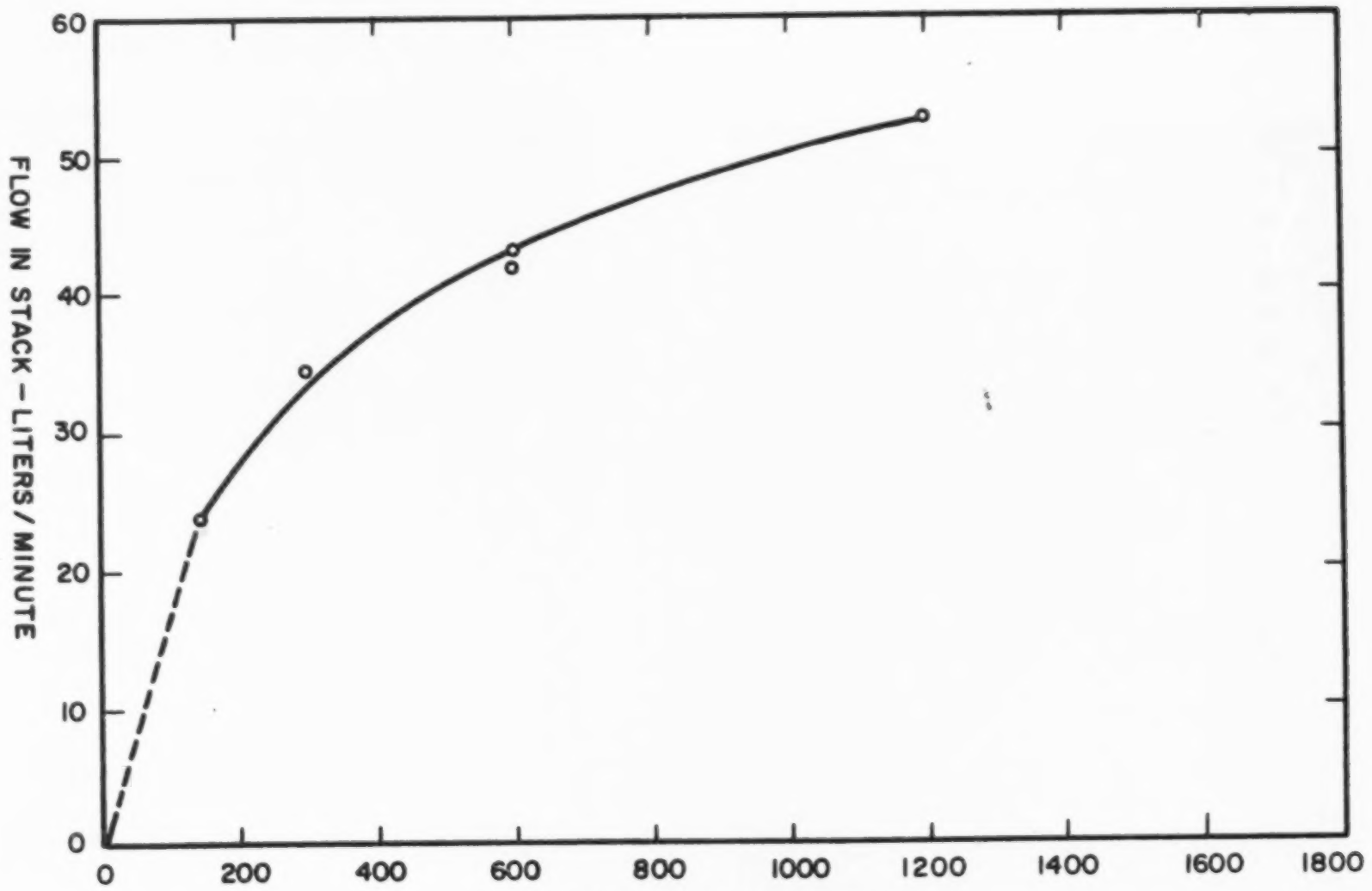

FIGURE 23

STACK FLOW VS AIR FLOW RATE

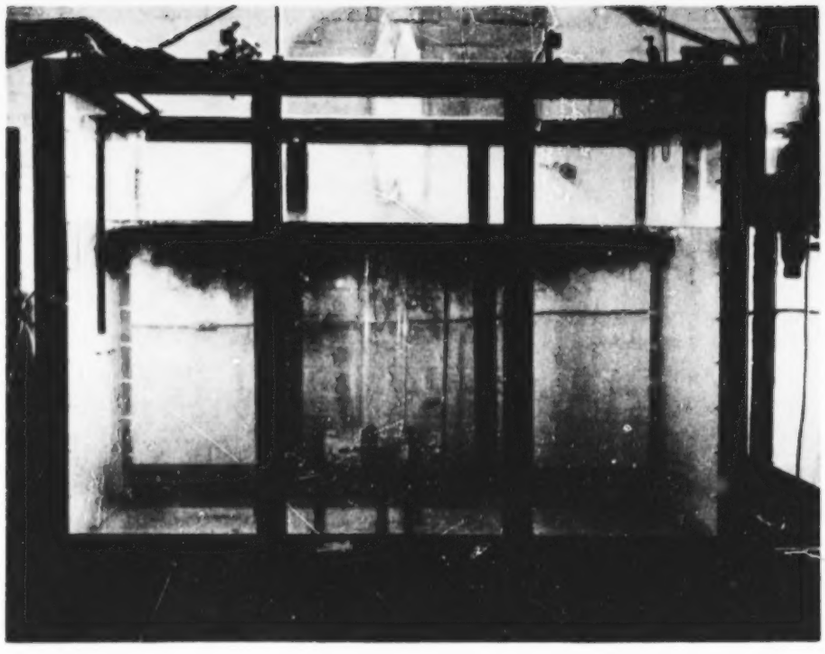

Photograph of Circulation Pattern. Solid Tracer: 10 sec.
Figure 24

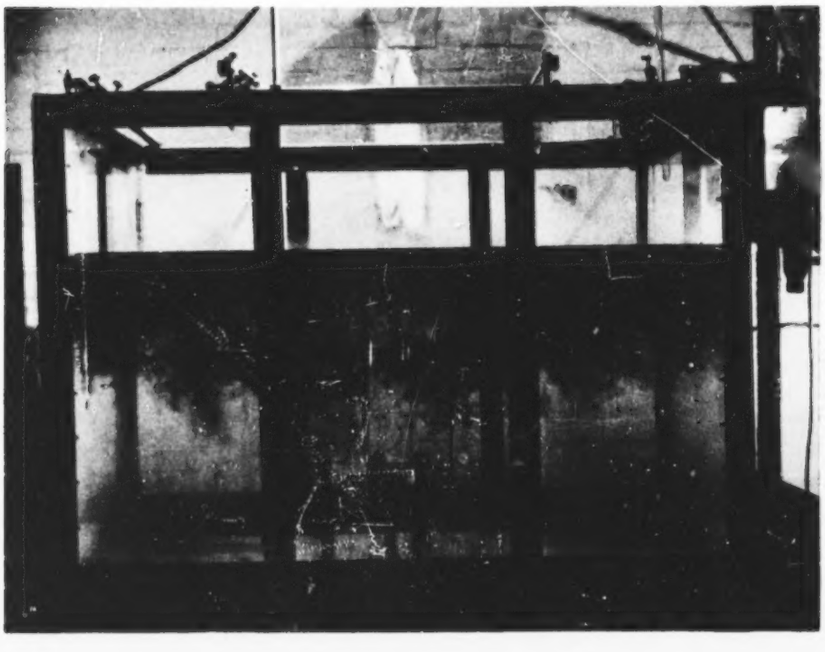

Photograph of Circulation Pattern. Solid Tracer: 30 sec.
Figure 25

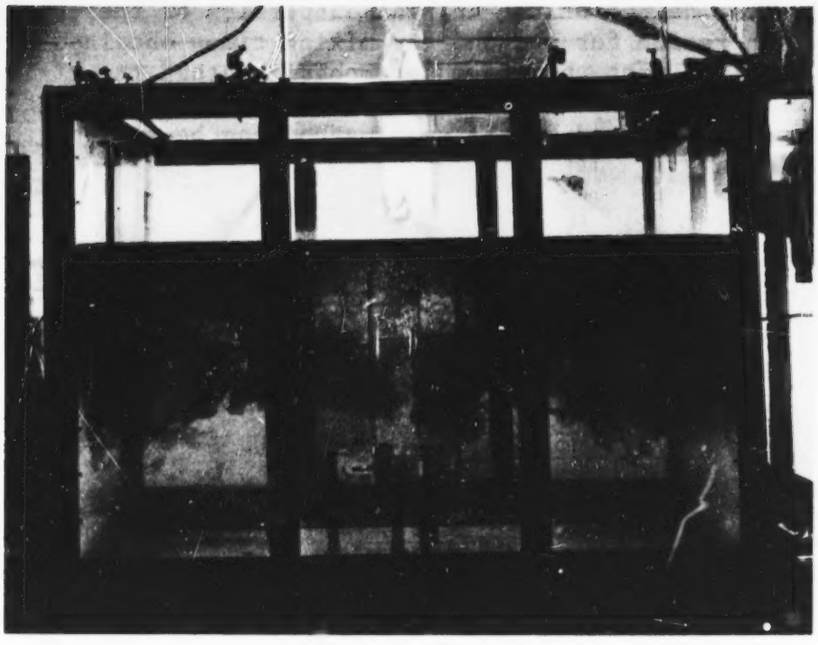

Photograph of Circulation Pattern. Solid Tracer: 1 minute
Figure 26

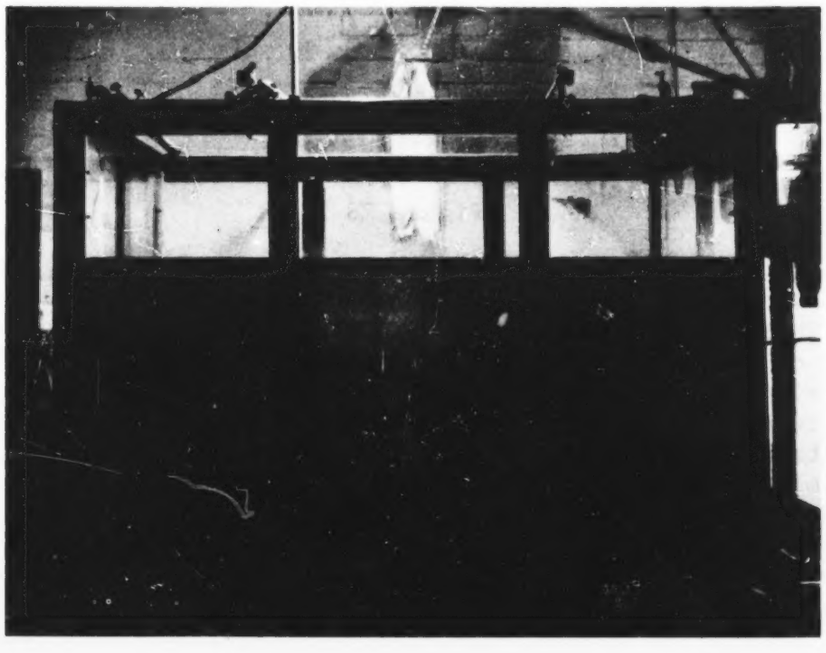

Photograph of Circulation Pattern. Solid Tracer: 2 minutes
Figure 27

The greater degree of the initial dispersion of the tracer seems to be the main reason for the shorter mixing times obtained by this tracer method. It must therefore be emphasized that the mixing time is not an absolute value but depends on the method of determination and only the results obtained by the same method can be subject to general correlation.

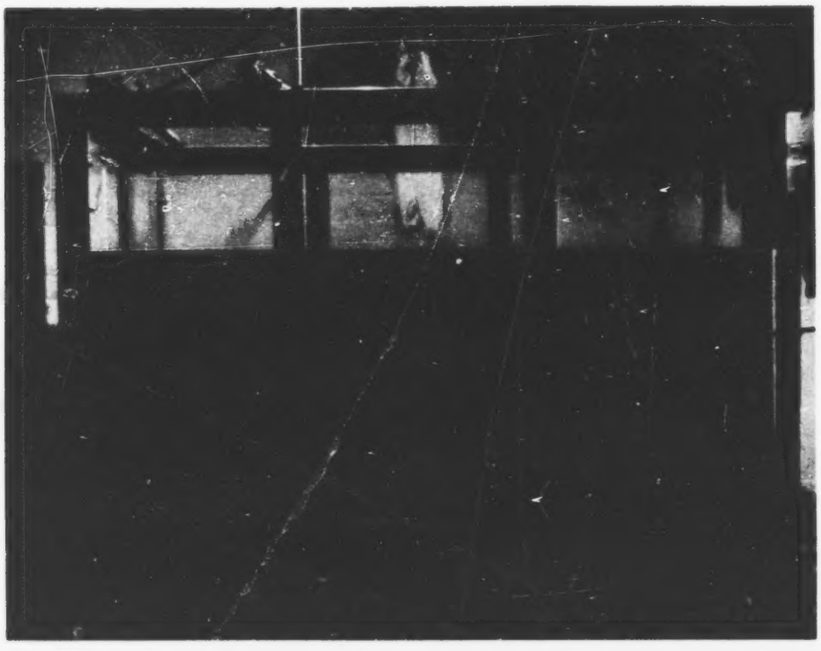

Photograph of Circulation Pattern. Solid Tracer: 3 minutes
Figure 28

It is of interest to note the sharp increase in the mixing time which can be seen in Figure 16 at an air flow rate between 150 and 300 cc/min. This sudden break in Figure 16 can be attributed to the magnitude of the currents generated in the mass of water. It can be expected that decreasing the rate of air flow some critical value would be reached at which the currents generated would not be sufficiently strong to establish a circulation of an appreciable magnitude in the whole body of water. Apparently at 150 cc/min. the system was handicapped in that the surface jet was unable to completely overcome the inertia of the stagnant body of water. Figure 17 (lower curve) which was obtained with the solid tracer technique, shows a similar break but of much smaller magnitude. This apparent discrepancy can be readily explained by the differences in the two tracer techniques which were discussed before. It may be expected a sharp transition of this

kind would occur independently of the tracer method used, although at different air flow rates.

Another important observation which can be made from Figures 16 and 17 is the spread of data which decreases with increased air flow rate. This is especially noticeable in Figure 16. In the case of the liquid tracer the probable error of a single determination was 8.6% at 2000 cc/min while at 150 cc/min it increased to 18%. This relatively poor reproducibility at low air flow rates is attributed to the smaller intensity and greater randomness of the generated water currents.

Preliminary studies of surface velocities conducted by hot film anemometers indicated values ranging from 1 ft/sec at 2000 cc/min of air to 0.3 ft/sec at 150 cc/min. It was further noted that the fluctuations in these velocities ranged from 25 to 50% with a tendency to increase at lower flow rates of air. In order to obtain some idea of the circulation pattern in the body of water, polystyrene beads were dropped in the tank and allowed to circulate freely. Except for the surface and the vertical jets, it was rather difficult to discern any definite flow pattern. Very little circulation was observed near the bottom of the tank, especially at the corners. Gay and Hagedorn (5) found in their work that a bottom layer approximately 1" thick was relatively unaffected by the mixing.

Efficiency of the Pumping Action of the Air Plume

The efficiency E of the air plume as a pump is defined, in this work, as the fraction of the net energy of the entering air E_n which is transformed into the kinetic energy E_k of water. The net energy of the air is expressed as the difference between the work of isothermal compression and the sum of the entrance, exit and frictional losses in the cylinder of the restricted system. Calculations showed that the energy losses caused by the presence of the cylinder were practically negligible (10% or less). The results are summarized in Table III.

$$E = \frac{E_k}{E_n}$$

Table III
Efficiency of the Restricted System

Air Flow Rate cc/min.	Efficiency E x 100
150	5.42
300	8.25
600	7.05

Although a direct comparison of the restricted system with that of a free rising plume is not fully justified, some interesting observations can be made from these figures. Kurihara (1, 10) in his studies (open plume) found a marked decrease in efficiency with decrease of the depth of submergence. The comparatively small efficiency in the present system might have been due to the very small height of the plume (1 1/4 - 2 1/2 ft as compared with 5 1/2 - 25 ft). Another point of interest is that under the same operating conditions (depth of water and air flow) the mixing times for both the restricted and unrestricted systems were practically identical. This was rather surprising because in the restricted system the water inflow from the side of the plume was absent whereas in the open plume it formed an essential part of the circulation pattern. There was therefore a considerable difference in the flow characteristics of the systems.

Average Mixing Time vs. Power Per Unit Volume

Figure 29 presents the mixing time as a function of the power input per unit volume. The power input was calculated by the equation:

$$H = Q_1 P_1 \ln \frac{P_1}{P_2}$$

where: H = Power

Q = Air flow rate

P = Absolute pressure

Subscripts 1 & 2 refer to initial and final conditions respectively.

Because for a given depth the power input is proportional to the air flow rate, the curve resembles closely Figure 16 where the mixing time was plotted against the air flow. The power per unit volume vs. mixing time correlation is of interest in scaling up model studies to large scale installations (see also Parker Ref. 15).

It is of interest to compare the magnitudes of the power per unit volume values obtained in this work with those of large-scale studies (Table IV). The comparison is only approximate because the degree of mixing was in this work considerably greater than in the large-scale tests where the only goal was to break thermal stratification. The data obtained in this research ranged from 10^{-6} to 1.3×10^{-7}. The difference in the order of magnitude can be due to the fact that in this research the contents of the tank were mixed close to the equilibrium concentration whereas in the large-scale tests this was not required. It is of interest to note that despite the wide differences in size and geometry of the model as compared with the reservoirs the difference in power input was not that great.

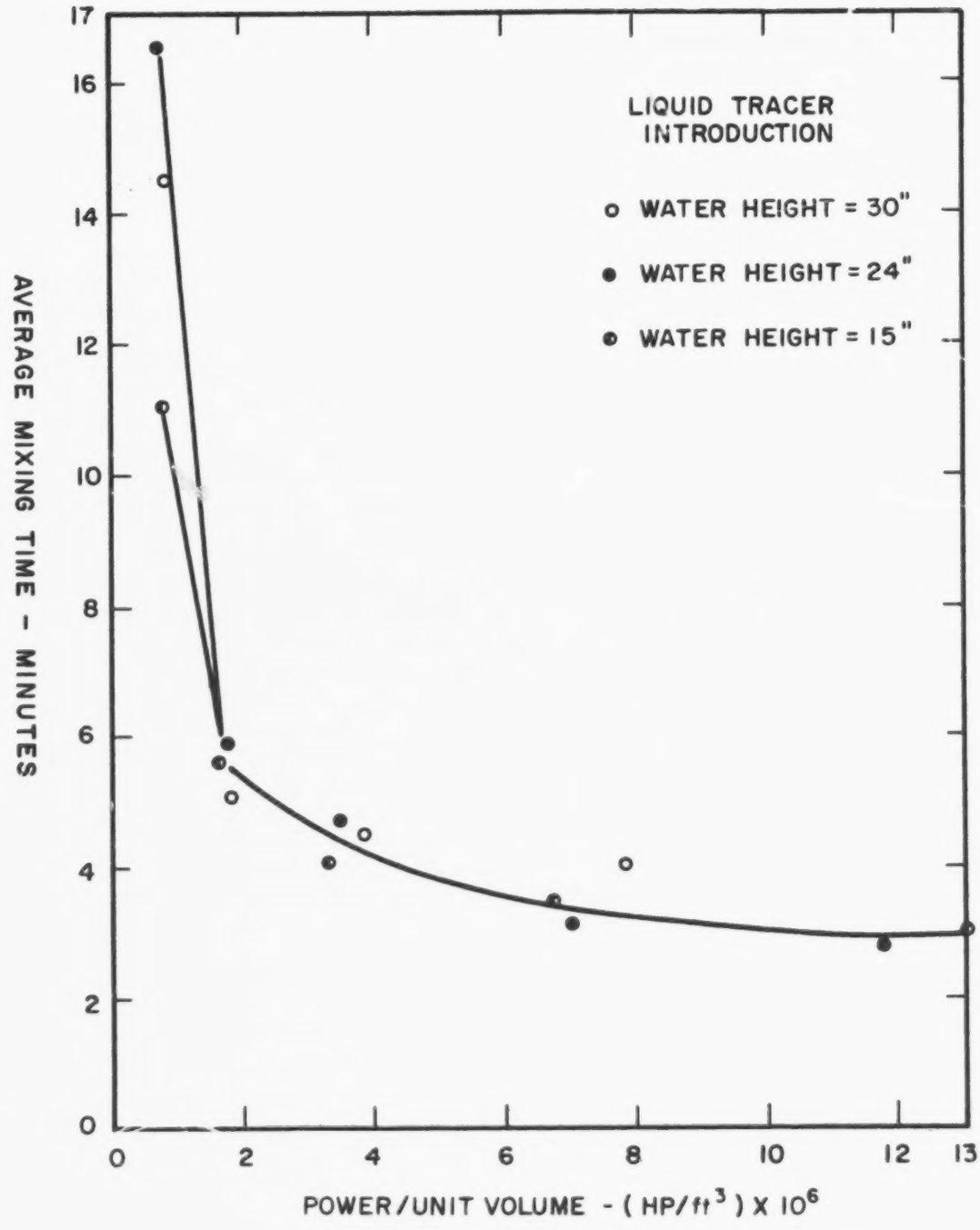

FIGURE 29

MIXING TIME VS POWER/UNIT VOLUME

Table IV
Diffused Air Mixing of Large Bodies of Water (21)

Reservoir	Volume ft^3	Power Input hp/ft^3
Indian Brook	13.8×10^6	5.8×10^{-7}
Wohlford	10.9×10^6	4.4×10^{-7}
Blelham Tarn	26.0×10^6	3.5×10^{-8}

Effect of Geometry on the Mixing Time

Figures 16 and 17, in addition to the effects of air flow rate, indicate also the effect of the geometry of the system on the mixing time. In this work the geometry is expressed in terms of the height of water level and location of the disperser.

It can be seen from Figure 16 that except for very low air flows (< 150 cc/min.) there was no apparent effect of water height on the mixing time. However, at 150 cc/min. and at a water height of 15 inches (curve B), the mixing time was about 20% lower than those for the other two heights (curve A). The lower curve of Figure 17 (solid tracer) shows a similar behavior indicating practically no effect of depth (15 and 24 inches) on the time of mixing. The effect of introducing the air at the side of the tank is shown by the two upper curves of Figure 17. For both the water depths used in this work, the side location of the air disperser resulted in longer mixing times. A similar behavior was also observed by Gay and Hagedorn (5). It can also be seen from Figure 17 that the effect of the side location of the disperser was more pronounced for the greater depth, resulting in longer mixing times for 24 inches as compared with 15 inches of water.

The adverse effect of the side location can probably be explained by the proximity of the wall and therefore its greater damping effect on the generated water currents as compared with the central location.

Limited data was also taken for two different disperser submergences at the same air flow rate and water depth. The results are shown in Table V.

It can be seen that the smaller the energy input (smaller submergence) the longer was the mixing time. In addition to the smaller energy input, the system with a disperser raised 13 cm off the tank bottom, was further handicapped in that the water level below the disperser was relatively stagnant and thus more resistant to the currents produced by the plume.

Table V
Effect of Disperser Submergence on Mixing Time

Air Flow cc/min	Depth of Disperser, cm	Water Height cm	Mixing Time min.
150	43	61	7.34
300	43	61	5.00
600	43	61	3.78
150	56	61	5.13
300	56	61	3.67
600	56	61	2.50

The above is in agreement with the observation of Gay and Hagedorn (5) who found that for a fixed flow rate of air, mixing was achieved more rapidly when the disperser was placed at the bottom of the tank rather than at an elevated position.

Effect of Bubble Size on the Pumping Capacity and the Mixing Time

Since the density of the plume depends on the air holdup and therefore on the velocity of rise of bubbles, it was expected that the small slowly rising bubbles should give a better pumping effect and therefore a shorter time of mixing.

Figures 30 and 31 show the effect of the bubble size (equivalent radius) on the pumping capacity and mixing time respectively.

The tests were conducted in the restricted system. The size of the bubbles was adjusted by introduction of a small amount of n-heptanol to reduce bubble coalescence (22). The largest bubble size was obtained by mounting over the disperser a small cap with a hole 1/32" in diameter. The mixing times were determined by means of the solid tracer.

It can be seen from Figures 30 and 31 that a 6-fold decrease in the bubble radius resulted in a 23% increase in the water flow and a 19% decrease in the mixing time.

Baines and Hamilton (1), studying the effect of orifice size on the surface jet velocity, found that a change in the orifice size from 0.10 to 0.30 cm had no effect. Similarly, Evans (4) in a study of pneumatic breakwaters noticed only a small change in the velocity of the surface jet when the bubble diameter was changed from 0.45 to 0.65 cm. Cyr (3),

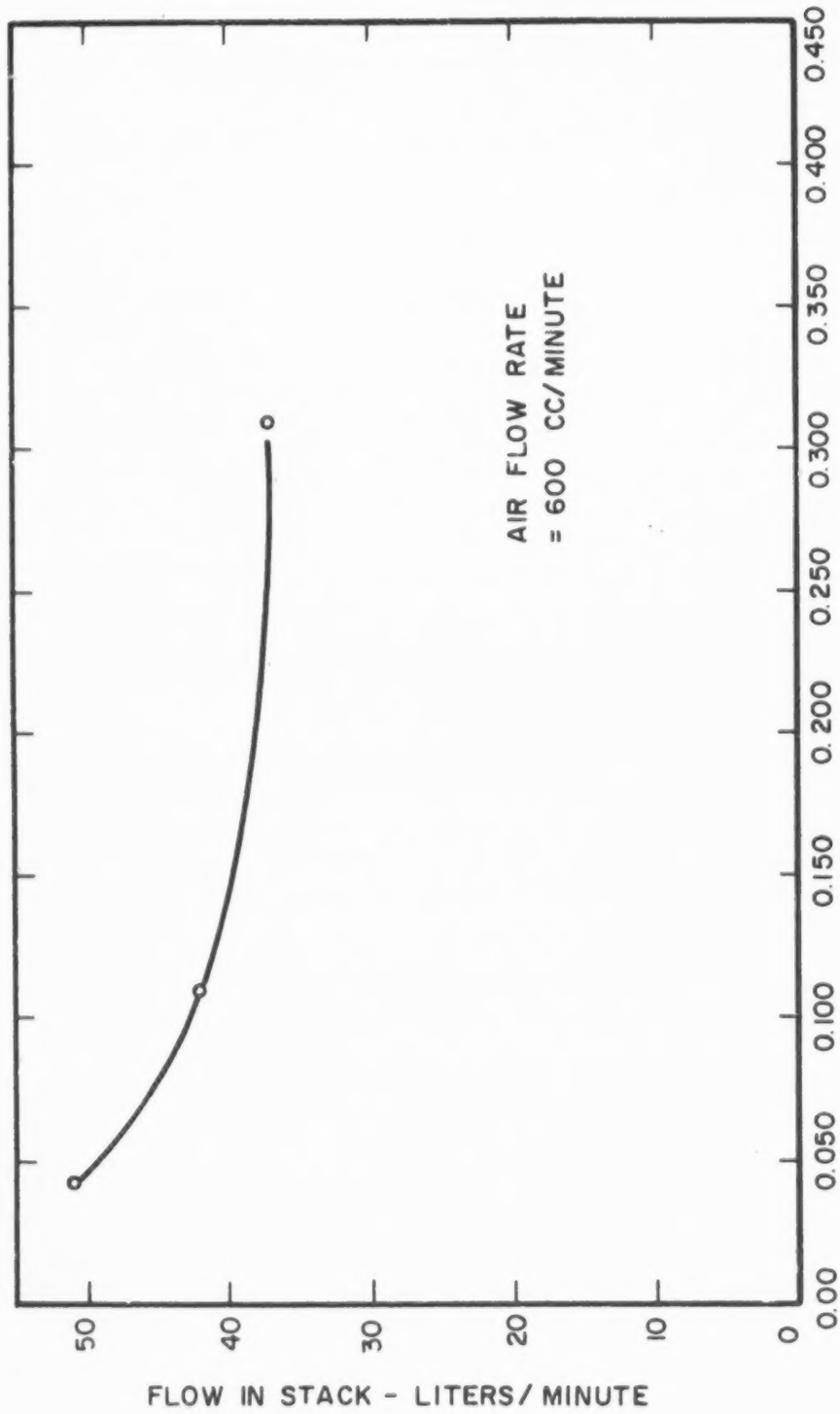

FIGURE 30

FLOW IN STACK VS BUBBLE SIZE

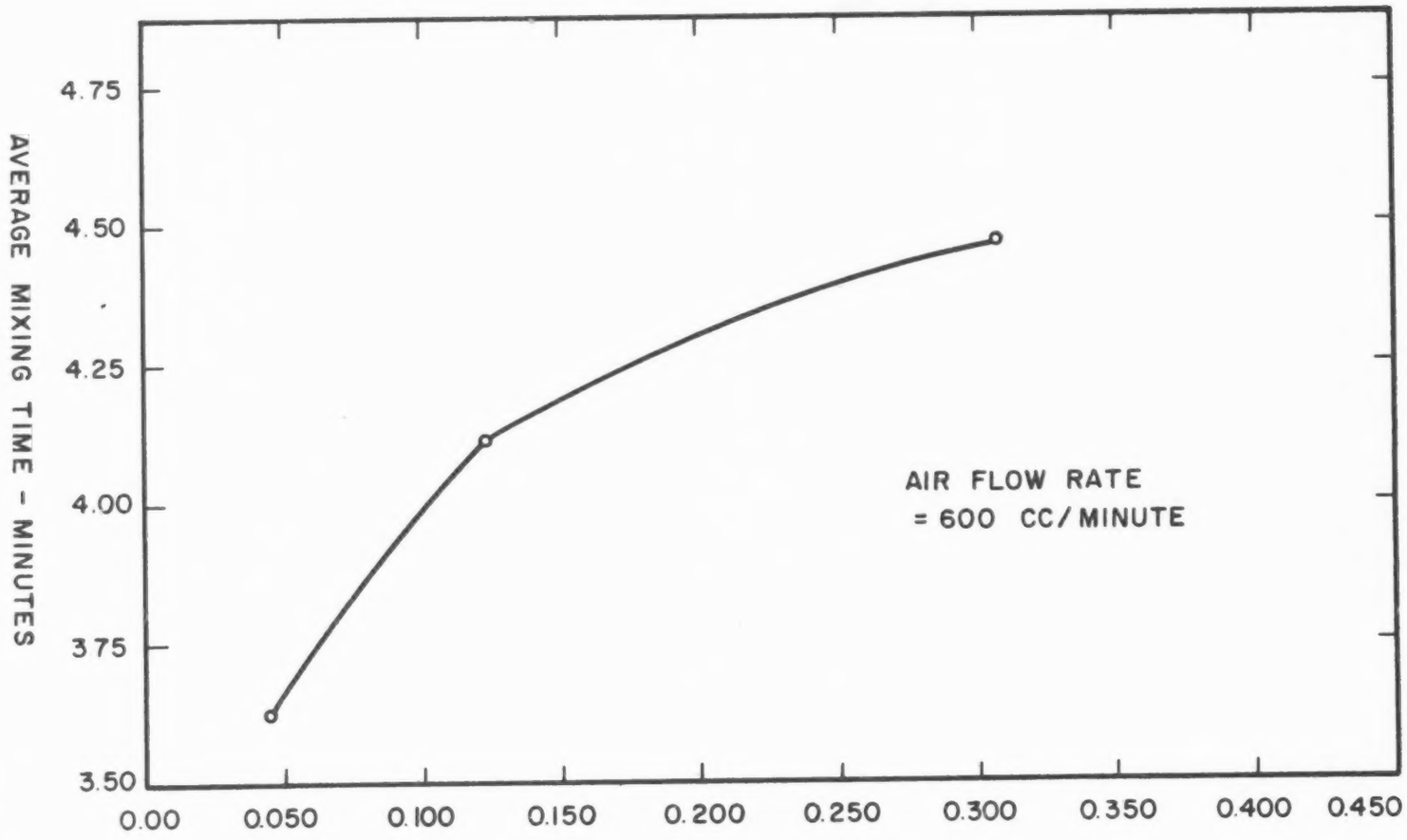

FIGURE 31

MIXING TIME VS BUBBLE SIZE

investigating the effect of process variables on the performance of a gas lift circulator found that a 25% increase in the water flow was obtained by decreasing the bubble radius from 0.33 to 0.04 cm.

Inspection of charts relating bubble velocities to their sizes (17, 6) shows that for bubble radii above the range of 0.06 to 0.08 cm the velocity of rise (and therefore the holdup) does not depend much on the bubble size. However, below this range the bubble velocity drops rapidly with the size of the bubbles resulting in a greater air holdup.

It is noted that for both the work of Baines and Hamilton (1) and Evans (4) the bubble sizes were in the region where the velocity of rise was relatively independent of size. Hence, no significant change in the pumping effect would be expected.

In the present research the bubble size was decreased to a radius less than 0.05 cm. Bubbles of this size have velocity of rise about 10 cm/sec while those having a radius of 0.3 cm, rise with a velocity almost three times as great (28 cm/sec). The smaller velocity of the bubbles used in this work, and the resulting increase in the residence time must have been the main factor responsible for the increased pumping effect.

Although the effect of bubble size on both the pumping performance and mixing time was not very great, it was, however, sufficiently pronounced to be considered as a design variable.

This point may be of special importance in the case where bubble coalescence occurs at the surface of the air disperser. Minute quantities of surfactants or other coalescence preventing agents would then have a marked effect on the size of the bubbles. A similar effect could be expected in solutions of inorganic salts (e.g. sea water) but at a higher concentration (23).

Correlation of Data

The experimental variables were correlated by means of Dimensional Analysis assuming isothermal operating condition. This last assumption was in agreement with the conditions of the work and at the same time gave the advantage of reducing the number of variables to those of essential importance in the system. The analysis resulted in the following relationship:

$$\Theta\left(\frac{g}{D}\right)^{1/2} = f\left(\frac{H}{D}\right)\left(Fr\right)^{1/2}$$

where: Θ = Mixing time, min.

g = Acceleration of gravity, cm/sec^2

D = Principal dimension of tank, cm

H = Height of water in tank, cm

Fr = Froude number, dimensionless.

The appearance of Froude number in the above equation is understandable since both inertia and gravitational forces are of primary importance in this system. The above correlation is shown graphically in Figure 32 in which the Froude number was defined as the densimetric Froude number expressed as (26):

$$Fr = \frac{Q/A}{\left(g \frac{\Delta\rho}{\rho w} H\right)^{\frac{1}{2}}}$$

where: Q = Air flow rate, cc STP/min

A = Cross section of tank, cm

$\Delta\rho$ = Density difference between water and plume, $^{gr}/_{cc}$

ρw = Density of water $^{gr}/_{cc}$

Although there is a considerable spread of data, this correlation shows a satisfactory relationship, especially when the small size of the tank is taken into consideration.

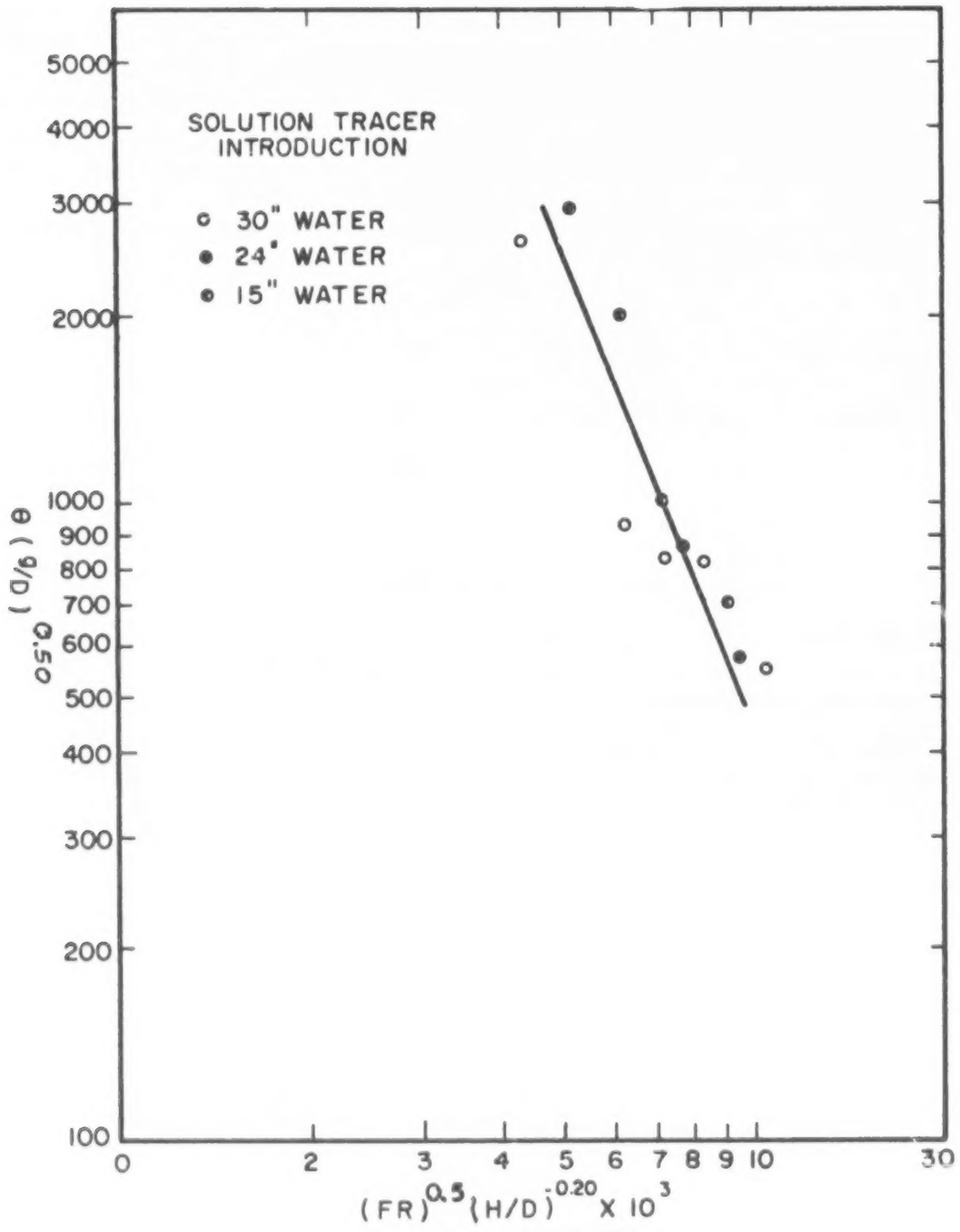

FIGURE 32

$\theta\left(\frac{g}{D}\right)^{0.50}$ VS $(FR)^{0.50}\left(\frac{H}{D}\right) - 0.20$

SECTION IV

References

1. Baines, W. D. and Hamilton, G. F., "On the Flow of Water Induced by a Rising Column of Air Bubbles," 8th Congress. Int. Assoc. of Hydraulic Res., Aug. 1959.

2. Cook, M. W. and Water, E. D., "Operational Characteristics of Submerged Gas Lift Circulators," U.S. Atomic Energy Commission, Dec. 1955.

3. Cyr, Steven, "Induced Air Circulation of Water," Unpublished M.S. Thesis, U. Maine, Orono, 1970.

4. Evans, J. T., "Pneumatic and Similar Breakwaters," Proc. Royal Soc., A231, 1955, p. 456.

5. Gay, F. and Hagedorn, Z., "Forced Convection in a Stratified Fluid by Air Injection," M.I.T. Thesis, Jan. 1962.

6. Haberman, W. and Morton, R. K., "An Experimental Investigation of the Drag and Shape of Air Bubbles Rising in Various Liquids," David Taylor Model Basin, U.S. Navy, Sept., 1953.

7. Harrel, J. E., "Mixing of Fluids in Small Diameter Tanks by Circulation," AEC Y-1531, April, 1966.

8. Hinze, J. O., "Turbulence," McGraw-Hill Book Co., New York, 1959, pp. 119-122.

9. Johnstone, R. E. and Thring, M. W., "Pilot Plant Models and Scale-up," McGraw Hill Book Co., New York, 1957, pp. 33-35.

10. Kurihara, M., "Pneumatic Breakwaters," Parts I, II, and III, Proc. of 1st Conferences on Coastal Eng. in Japan, Nov., 1954.

11. Lamont, A. G. W., "Air Agitation and Pachuca Tanks," Can. J. of ChE., Aug. 1958, pp. 153-160.

12. Morton, B. R., et al, "Turbulent Gravitational Convection from Maintained and Instantaneous Sources," Proc. Royal Soc., 234A, Jan. 1956, pp. 1-23.

13. Nevers, Noel De, "Bubble Driven Fluid Circulations," AIChE J., March, 1968, pp. 222-226.

14. Nickerson, H., "Gloucester-Forced Circulations of Babson Reservoir," Div. of San. Eng., Mass. Dept. of Health, Boston, 1960.

15. Parker, N. H., "Mixing," ChE, June 8, 1964, pp. 165-220.

16. Riddick, T. M., "Forced Circulation of Reservoir Waters," Water and Sewage Works, Vol. 104, No. 6, June, 1957, pp. 231-237.

17. Rosenberg, B., "The Shape and Drag of Air Bubbles Moving in Liquids," Report 727 Navy Dept., Sept., 1950.

18. Straub, L. G., and others, "Experimental Studies of Pneumatic and Hydraulic Breakwaters," U. Minn., St. Anthony Falls Hydraulic Lab., Tech. Paper No. 25, Series B, Aug., 1959.

19. Taylor, G., "The Action of a Surface Current Used as a Breakwater," Proc. Royal Soc., A231, 1955, pp. 467-478.

20. Thermal Systems, Inc. Bulletin TB5, St. Paul, Minn.

21. U. S. Dept. of H.E.W., Public Health Service, "Water Qualities Behavior in Reservoirs," compiled by J. Symons. (1969)

22. Zieminski, S. A., et al, "Behavior of Air Bubbles in Dilute Aqueous Solutions," Ind. Eng. Chem., May, 1967, pp. 233-242.

23. Zieminaki, S. A. and Whittemore, R.C., "Behavior of Gas Bubbles in Aqueous Electrolyte Solutions," ChE. Sci., Publication Pending.

24. Zlokarink, M., "Homogenisieren von Flussigkeiten durch Aufsteigende Gasblasen," Chem. Ing.-Techn., 40, 1968, pp. 765-769.

25. Bryan, J. G., "Improvement in the Quality of Reservoir Discharges Through Reservoir Mixing and Aeration," R. A. Taft San. Eng. Center, Cinn., Ohio, April 3-5, 1963, PHS Publ. No. 999-WP-30, June 1965, pp. 317-34.

26. King, D.L., "Hydraulics of Stratified Flow," Report No. Hyd-563, Hydraulics Branch, Division of Research, U. S. Dept. of Interior, June 3, 1966.

1 Accession Number	2 Subject Field & Group	SELECTED WATER RESOURCES ABSTRACTS INPUT TRANSACTION FORM
	05G	

5 Organization

University of Maine, Orono, Maine 04473

6 Title

INDUCED AIR MIXING OF LARGE BODIES OF POLLUTED WATER

10 Author(s)

Stefan A. Zieminski
and
Raymond C. Whittemore

16 Project Designation

16080DWP11/70

21 Note

22 Citation

23 Descriptors (Starred First)

Aeration,* Water Quality Control,* Air Entrainment, Air Bubbles, Coalescence

25 Identifiers (Starred First)

Air Plume, Diffusion, Bubble Size, Energy Input, Mixing, Tracer, Mixing time.

27 Abstract

The work discussed in this report constitutes the Phase I of the investigation of induced air mixing of large bodies of water. The objective of this work was to conduct a pilot scale study to estimate the effects of variables such as the air flow rate, geometry of the body of water, energy input, size of air bubbles, and the pumping capacity of the air plume on the time of mixing. The latter was defined as the time required to reach 90% of the equilibrium concentration of the KCl tracer. In the study emphasis was put on the direction and relative magnitudes of the variables in order to obtain guidelines for large-scale investigation. Considerable time was spent on the development of the various experimental techniques. The tests were conducted in a plexiglas tank of 180 gallons capacity. It is stressed that the induced air system was investigated only from the viewpoint of its mixing performance. Its effect on aquatic life was not considered in this work.

Abstractor S. A. Zieminski

Institution University of Maine, Orono, Maine 04473

WR:102 (REV. JULY 1969)
WRSIC

SEND TO: WATER RESOURCES SCIENTIFIC INFORMATION CENTER
U.S. DEPARTMENT OF THE INTERIOR
WASHINGTON, D. C. 20240

* GPO: 1969-359-339